PolyPublie
Polytechnique Montréal

POLYTECHNIQUE MONTRÉAL
UNIVERSITÉ D'INGÉNIERIE

Titre: Title:	Doped SiO thin films for integrated optics and microelectronics
Auteur: Author:	Pengnian Shen
Date:	1991
Type:	Mémoire ou thèse / Dissertation or Thesis
Référence: Citation:	Shen, P. (1991). Doped SiO thin films for integrated optics and microelectronics [Mémoire de maîtrise, École Polytechnique de Montréal]. PolyPublie. https://publications.polymtl.ca/56728/

Document en libre accès dans PolyPublie
Open Access document in PolyPublie

URL de PolyPublie: PolyPublie URL:	https://publications.polymtl.ca/56728/
Directeurs de recherche: Advisors:	John F. Currie, & S. Iraj Najafi
Programme: Program:	Génie physique

Ce fichier a été téléchargé à partir de PolyPublie, le dépôt institutionnel de Polytechnique Montréal
This file has been downloaded from PolyPublie, the institutional repository of Polytechnique Montréal

https://publications.polymtl.ca

UNIVERSITÉ DE MONTRÉAL

DOPED SiO_2 THIN FILMS FOR INTEGRATED OPTICS AND MICROELECTRONICS

par

Pengnian SHEN
DÉPARTEMENT DE GÉNIE PHYSIQUE
ÉCOLE POLYTECHNIQUE

MÉMOIRE PRÉSENTÉ EN VUE DE L'OBTENTION
DU GRADE DE MAITRE ES SCIENCES APPLIQUÉES (M.Sc.A.)

août 1991

© Pengnian Shen 1991

National Library of Canada

Bibliothèque nationale du Canada

Canadian Theses Service

Service des thèses canadiennes

Ottawa, Canada
K1A 0N4

The author has granted an irrevocable non-exclusive licence allowing the National Library of Canada to reproduce, loan, distribute or sell copies of his/her thesis by any means and in any form or format, making this thesis available to interested persons.

L'auteur a accordé une licence irrévocable et non exclusive permettant à la Bibliothèque nationale du Canada de reproduire, prêter, distribuer ou vendre des copies de sa thèse de quelque manière et sous quelque forme que ce soit pour mettre des exemplaires de cette thèse à la disposition des personnes intéressées.

The author retains ownership of the copyright in his/her thesis. Neither the thesis nor substantial extracts from it may be printed or otherwise reproduced without his/her permission.

L'auteur conserve la propriété du droit d'auteur qui protège sa thèse. Ni la thèse ni des extraits substantiels de celle-ci ne doivent être imprimés ou autrement reproduits sans son autorisation.

ISBN 0-315-72762-4

Canadä

UNIVERSITÉ DE MONTRÉAL

ÉCOLE POLYTECHNIQUE

Ce mémoire intitulé:

DOPED SiO_2 THIN FILMS FOR INTEGRATED OPTICS
AND MICROELECTRONICS

présenté par: Pengnian Shen

en vue de l'obtention du grade de: MAITRE ES SCIENCES APPLIQUÉES (M.Sc.A.) a été dûment accepté par le jury d'examen constitué de:

Michel. R. Wertheimer .... Ph.D., Président

John. F. Currie .... Ph. D.

Iraj. S. Najafi .... Ph.D.

Ludwik. Martinu .... Ph.D.

SOMMAIRE

Ce travail consiste à étudier, d'une part, la caractérisation optique et mécanique de couches minces de SiO_2, pures et dopées, fabriquées avec la technique de déposition en solution, et d'autre part, l'application de telles couches en microélectronique et en opto-électronique.

La première partie de ce mémoire est consacrée au procédé de "Spin-on"; les paramètres expérimentaux permettant la production de couches minces de bonne qualité y sont identifiés. L'indice de réfraction et l'uniformité du dépôt sont les principales caractéristiques du film ayant été optimisées.

La caractérisation optique a été effectuée avec un système Leitz de spectrométrie par réflectance spécialisé dans les couches minces, lequel mesure la réflectance normalisée avec une grande précision. Nous avons utilisé une approche analytique et numérique basée sur la méthode de la matrice caractéristique pour traiter les données sur la réflectance et nous avons ainsi obtenu l'épaisseur et l'indice de réfraction du film avec une très bonne précision, dépassant les posibilités du logiciel livré par Leitz avec ce produit.

Cette approche a aussi permis la généralisation des mesures de réflectance aux cas où le film et le substrat sont, indépendamment l'un de l'autre, transparents ou absorbants.

Dans la seconde partie de ce mémoire, la methode dévelopée en première partie est appliquée à la caractérisation de dépôts de SiO_2 sur trois semi-conducteurs importants: le Si, le GaAs et le InP. Les propriétés mécaniques et l'homogénéité de chacun des dépôts sont également mesurées et analysées.

Puisque les films de SiO_2 dopés fabriqués par la méthode de "Spin-on" peuvent servir à la fois de guide d'onde à indice gradué, de traitement antiréflection de surfaces de verre ou de semiconducteurs, ou de couche protectrice sur des surfaces métalliques, nous avons consacré la troisième partie de ce travail à la caractérisation du dopage des couches de SiO_2 avec du TiO_2, du P_2O_5-In_2O_3 et du Coumarin 504.

Du SiO_2 est dopé avec du Coumarin 504 et on en recouvre la surface d'un guide d'onde de verre. On démontre ensuite avec ce nouveau guide la fluorescence caractéristique dans le domaine de longueurs d'onde allant de 520 nm à 570 nm.

ABSTRACT

This work is directed to the optical and mechanical characterisation of solution deposited pure and doped SiO_2, and to its application in microelectronics and optoelectronics.

First we studied the spin-on process and identified principal process parameters required for reproducible production of high quality optical coatings. The basic film characteristics which were optimised were the optical index of refraction and the thickness uniformity.

Optical characterisation was performed using a state of the art reflectance spectrometry system (Leitz MPVSP) applied to thin films for the measurement of normalised reflectance with high accuracy. We have developed an analytical and numerical approach to the reflectance data based on the characteristic matrix method. This approach allows us to obtain the film thickness and optical constants with a high accuracy, surpassing the software capabilities supplied by Leitz with this product.

Using our techniques, we have been able to extend measurements of the normalised reflectance spectra to both

transparent and absorbing thin films and to either transparent or absorbing substrates.

In the second part of this thesis we apply our method to the characterisation of SiO_2 films deposited onto three different semiconductor substrates: Si, GaAs and InP. For all three substrates, the films' mechanical properties and uniformity were measured and analysed.

Spin-on SiO_2 films can be used as index-graded light-guiding, as anti-reflection coatings on glass and semiconductor surfaces, and also as a protective coatings for thin metal films. The third part of the work is devoted to the characterisation of SiO_2 layers doped with TiO_2, P_2O_5, and In_2O_3. The Coumarin 504 is successfully used as a dopant in spin-on SiO_2 and overlay on top of a glass waveguide. It shows the characteristic fluorescence in the wavelength range of 520-570 nm.

ACKNOWLEDGEMENT

The research work presented in this thesis was completed under the supervision of Professor John F. Currie, to whom I express my sincere gratitude, appreciation for his kindness, guidance, encouragement and support.

I am also indebted to professor Iraj S. Najafi, codirector of this work, for his help, encouragement and support.

Thanks are to the professors and other members of the Department of Engineering Physics for their help and friendly atmosphere during the period of this work.

I thank to Dr. Ludwik. Martinu for helpful discussions on the application of the reflectance method to absorbing films.

Assistance in the measurement of the glass waveguiding properties by Mr. Weijang. Wang , Ph.D student at the Department of Engineering Physics, is appreciated.

Financial assistance for this work was made available through the Groupe des Couches Minces and the FCAR Electronics and Photonics Team grant. Finally, tuition financial assistance received from the Service des Études Supérieures is gratefully acknowledged.

CONTENTS

Page

Sommaire ....(iv)

Abstract ....(vi)

Acknowledgment ....(viii)

Contents ....(ix)

List of figures ....(xi)

Chapter 1. Introduction ....(1)

Chapter 2. Method of Preparation of Solution Deposited

Thin Films ....(8)

Chapter 3. Determination of the Film Thickness and

its Index of Refraction ....(14)

3.1. Determination of Refractive Index and Thickness

of Solution Deposited Thin Films on Silicon

and Glass ....(14)

3.2. Normalised Reflectance of Absorbing Films on

Absorbing or Transparent Substrates ....(35)

3.3. Experimental Use of the Normalised Reflectance

Method ....(43)

Chapter 4. Solution Deposited SiO_2 on Si, GaAs and InP ....(47)

Chapter 5. Mechanical Properties and Film Homogeneity ....(58)

5.1. Film Homogeneity ....(59)

5.2. Tensile Stress ....(67)

Chapter 6. Antireflective, Protective and Waveguide

Applications ....(73)

7. Conclusion ....(90)

Bibliography ....(95)

Appendix ....(103)

Appendix 1.Optical Constants of Si, GaAs and InP...............................(104)

Appendix 2. The Normalised Reflectance Minima

of Thin Films of Different Refractive Index on

Si, GaAs and InP ....(108)

Appendix 3. The Multi-layer Transparent Thin

Films on Semiconductors ....(113)

Appendix 4. The Single Transparent Film on a Transparent

Substrate ....(117)

Appendix 5. The Single Transparent Film on an Absorbing

Substrate ....(121)

LIST OF FIGURES

page

Fig.2.1- The heat treatment of solution deposited films, showing the temperature cycle ....(12)

Fig.3.1- Normalised reflectance of a thin SiO_2 film with n_f=1.42 on a thick silicon substrate at a wavelength of 400 and 600 nm ....(17)

Fig.3.2- Normalised reflectance minimum and wavelength relations for films of different refractive index ranging from 1.40 to 1.80 on a silicon substrate ....(19)

Fig.3.3- The R_{norm}-λ curve of transparent film 400 nm thick with a refractive index of 1.42 ....(20)

Fig.3.4- R_{norm} (554 nm)-R_{norm} (660 nm) at different film thickness for a film of n_f=1.42 on silicon substrate ....(22)

Fig.3.5- Air, film, substrate assembly ....(23)

Fig.3.6- R_{norm}-$d_f n_f$ relations of films with different refractive index ....(27)

Fig.3.7- Example, normalised reflectance for films of different thickness of 100, 200 and 300 nm and index of refraction n_f=1.7 on glass ....(28)

Fig.3.8- The $R_{norm,minimum}$ or $R_{norm,maximum}$ and wavelength relations for various film refractive index values on glass ....(29)

Fig.3.9- Practical air-films-substrate-air assembly ....(31)

Fig.3.10- R'_{norm}, R_{norm} and R'/R, R'_0/R_0-I curves of a transparent film with n=1.7 and d=300 nm on glass substrate ....(34)

Fig.3.11- Refractive index of the thermaly grown SiO_2 on silicon ....(44)

Fig.3.12- Simulated and experimental normalised reflectance of a thermally grown SiO_2 of 857.5 nm on silicon ....(45)

Fig.4.1- The calculated normalised reflectance spectrum of SiO_2 films with thickness ranging from 5 to 30 nm on a silicon substrate ....(51)

Fig.4.2- The calculated normalised reflectance spectrum of native oxide with thickness ranging from 5 to 30 nm on a InP substrate ....(52)

Fig.4.3- Measured refractive index of spin-on SiO_2 film deposited on Si ....(54)

Fig.4.4- Refractive index of solution deposited SiO_2 films doped with TiO_2 and baked at 300 °C ....(55)

Fig.5.1- Thickness uniformity of a solution deposited silicon dioxide film on a 2" silicon wafer ....(60)

Fig.5.2- Thickness uniformity of a solution deposited SiO_2-TiO_2 film on a 2" silicon wafer ....(60)

Fig.5.3a- The air-film-substrate assembly and its refractive index ....(63)

Fig.5.3b- Calculated normalised reflectance as a function of wavelength for a film with thickness d=360 nm and n_m=1.4 for two different values of $\Delta n/n_m$ of 7% and -7% on silicon substrate ....(64)

Fig.5.4- The film inhomogeneity in the vertical direction and the normalised reflectance relationship for solution deposited SiO_2 on silicon ......(66)

Fig.5.5- Plasma etch rate of silicon dioxide films baked at different temperature ......(69)

Fig.5.6- Plasma etch rate of silicon dioxide-titanium dioxide films ......(71)

Fig.6.1- Two layer anti-reflection layer on glass ......(75)

Fig.6.2- Single layer anti-reflection film on silicon ......(76)

Fig.6.3- Normalised reflectance of SiO_2 film on aluminium ......(78)

Fig.6.4- Normalised reflectance spectrum of SiO_2-TiO_2-glass assembly with SiO_2-TiO_2 layer thickness of 153 nm ......(81)

Fig.6.5- Absorption spectrum of a waveguide with Coumarin doped SiO_2 overlay ......(83)

Fig.6.6- System used for measurement of waveguide spectrum characteristics ......(84)

Fig.6.7- Fluorescence spectrum of a waveguide with Coumarin doped SiO_2 overlay ......(85)

Fig.6.8- The processing temperature and film thickness relations of a 1.25:1 P_2O_5/In_2O_3 thin films ....(87)

Fig.6.9- Dispersion curve of solution deposited 1.25:1 P_2O_5/In_2O_3 thin films ....(88)

Fig.6.10- Normalised reflectance spectrum of a 234.8 nm thick P_2O_5/In_2O_3 film on Si substrate ....(89)

CHAPTER 1

INTRODUCTION

Silicon dioxide is one of the most important dielectric materials. During the nineteen sixties a great deal of original work was done on its application to planar microelectronics technology on silicon in such diverse situation as dielectrics, diffusion masks and passivation layers [1.2]-[1.4], [1-7]-[1-9], [1-12].

Five deposition methods have been extensively studied: thermal oxidation, sputtering, chemical vapour deposition, vacuum evaporation [1.15] and anodic oxidation [1.13].

In the early seventies, two important breakthroughs in optoelectronics and optical communication have been accomplished: the semiconductor laser and the low loss glass optical fiber. Ever since silicon dioxide films were studied in the context of integrated optics, and in particular for planar waveguide on Si substrates [1.10] and on other transparent substrates [1.14].

The origins of optical thin films predate microelectronics, when in 1886 Rayleigh reported that a high refractive index thin

film layer can serve as an anti-reflection coating on a glass substrate [1.6]. It was only when high vacuum technology developed in the nineteen thirties, and reproducible production of optical thin films became possible.

Another early film production technology was that of chemical solution coating. The alkyl oxides of silicon or titanium are readily produced and purified [1.1]. At first the solution deposited pure and doped SiO_2 thin film coatings were used as antireflection coatings (AR) on glass and semiconductors, and as multilayer antireflection coatings for distinct wavelength ranges [1.5,1.16]. Later, this technology was used to make waveguiding layers on glass with inorganic and organic (including photoresists and epoxy [1.11]) thin films. The chemical solution method, with its ease of doping at low processing temperatures (200-500°C) and its planarisation capability, is readily combined with other processes in microelectronics or optoelectronics.

For example, it has been reported that the inorganic silicon dioxide films doped with lead oxide can be produced by mixing two commercially available organic solutions, and be directly applied to the glass substrate. Then they are cured at very low temperature of

$60^{o}C$ to obtain a low loss planar waveguide (0.3 dB/cm at 1.064 μm) [1.11]. Similarly, Ti doped, solution deposited SiO_2 films, first studied as antireflection (AR) layers, also proved to be a waveguiding material [1.17,1.18], and already several commercial products have appeared.

The work presented here is focused on the study of solution deposited SiO_2 and TiO_2 films and their application to integrated optics and microelectronics. To ensure a full control and reproducibility of the films with same properties, we have first studied the solution deposition process itself. The ultimate measure of the success of the deposition technique is the optical quality of the film, and we have developed here an accurate method to measure the film thickness, refractive index, uniformity, and film depth homogeneity, and experiments were done for both absorbing and transparent substrates.

In Chapter 2 we review various methods for preparation of thin SiO_2 and TiO_2 films by solution methods with emphasis on the spin-on method, and their compatibility with microelectronics processing. Their processing parameters and the resulting film index and thickness relations are studied.

TiO_2 films and TiO_2 doped SiO_2 are important. Solution deposited TiO_2 has a refractive index of 2.0-2.1[1.18]. When mixed with SiO_2, films with different refractive indices and index gradients can be manufactured to obtain special antireflection and waveguiding properties. TiO_2 films have unique mechanical properties as well, but they require special characterisation.

Chapter 3 is devoted to the development of a practical measurement technique for film refractive index and thickness evaluation, based on normalised reflectance. To be versatile enough, we provide the mathematical expressions for both transparent and absorbing substrates in Sec.3.1.

In Sec.3.2 we generalise our mathematical treatment to both multilayer and weakly absorbing films and indicate how to calculate practically most easily and accurately. Some experimental results are shown in Sec.3.3 to illustrate the use of our method, and the evaluation of the refractive index of thermally grown SiO_2 on silicon to verify the accuracy of the method.

Some particularities for thin SiO_2 and TiO_2 films on semiconductor substrates (Si,GaAs,InP) are studied in Chapter 4. Nevertheless, the general mathematical techniques of Chapter 4

can be applied to any semiconductor substrate whose optical properties are known.

The films mechanical properties and optical homogeneity are treated in Chapter 5. The in plane homogeneity is measured from point by point using a focused optical beam, and the in depth homogeneity is measured using the normalised reflectance spectrum and our mathematical models introduced in Chapter 3.

Chapter 6 is devoted to three applications of the solution deposited SiO_2 films: antireflection films, protective coatings and planar waveguides.

In order for the results of the mathematical modelling of Chapter 3 to be easily used for practical day-to-day characterisation and for simulation in the laboratory we have included five appendices. These appendices provide a practical procedure for thin film analysis for various film and substrate configurations.

The optical constants of three semiconductors studied in Chapter 4 and in wide use in the laboratory (Si, GaAs and InP) are listed in Appendix 1. Curves for the normalised reflectance minimum and refractive index relations for single transparent film layers on

Si, GaAs and InP are presented in Appendix 2. Combining the two appendices and using MATHCAD software, one can calculate the reflectance minima of the transparent films on three important semiconductors. The equations used are described in Sec.3.1.

The general treatment presented in Sec.3.2 can be used under various circumstances. As an example, we present an 8 layer simulation software in Appendix 3 which, after some revision, can be adapted to treat other similar multilayers.

Appendix 4 and Appendix 5 present software for normalised reflectance spectrum calculation for a transparent single layer both on an absorbing and a transparent substrate.

In this work we have used the solution method to fabricate pure and doped SiO_2 thin films which can ultimately be used in optoelectronics and microelectronics processing. The normalised reflectance method is introduced and a practical software for this purpose is developed. Although spin-on films on Si are widely studied, we are among the first to characterise them on GaAs, InP and on glass. For the first time, we have addressed the problem of film inhomogeneity and provided a means to treat it analytically and numerically. We have shown as well that for the special case of

linearly inhomogenious films, the refractive index obtained from the refractive minimum is the mean refractive index.

We have successfully incorporated organic dye (Coumarin 504) into the SiO_2 film and used it as an overlay on glass waveguides. We have demonstrated light coupling and fluorescence in the overlayed glass channel waveguide.

In developing the P_2O_5 doping method, we have produced a novel transparent 1:1.25 In_2O_3/P_2O_5 material in the form of a thin film and have measured its refractive index and pointed out its potential application as a dielectric and waveguiding materials.

CHAPTER 2

METHOD OF PREPARATION OF SOLUTION DEPOSITED THIN FILMS

Several methods can be used to deposit oxide films from solution. SiO_2, TiO_2, ThO_2 and In_2O_3 are deposited with organic solutions of alkyl oxide, nitrate or butyrate as starting materials [2.1]. Solution deposition was originally developed for coating large surfaces with antireflection coatings, often by dipping. As the interest in thin film waveguides arose, new coating methods had to be adapted [2.2]. In the early solution deposited waveguide experiments, puddles of organic solution were formed on horizontal surfaces, and the excess solution was removed by run-off, holding the substrate in vertical position. Films were then cured at a temperature between 50-200° C. Depending on the solution types, film thicknesses in the range of 0.8-2.0 μm were obtained. Unfortunately, with this technique the film thickness is uniform only in the center part of the substrate [2.2]. Later both the spin-on and a slow-removal method were used to improve thickness

uniformity. In all these techniques, the optical properties of the films are very process dependent [2.3].

The temperature cycling sequence, the solution composition, the spinning speed in the spin-on method, and the extraction speed in the dipping method all influence the resulting films' properties.

The dipping method is double sided and requires a stable mechanical structure without vibration. It is best suited for large surface coating. Process standardization can deliver reproducibly good refractive index and thickness uniformity [2.3]. The spin-on method is single sided, and although it is not meant for very large surface coating, it is compatible with the microelectronics processing. In the present work, the spin-on method is used exclusively.

The substrates used are 1 mm thick Fisher microscope slides, Corning 0211 glass, Si, GaAs and InP. The substrates are cleaned before coating. For glass or SiO_2 we use a mild liquid detergent for the substrate cleaning, followed by DI water (18 MΩ), iso-propanol, acetone, TCE (tri-chloro-ethylene), acetone, propanol consecutively. For the Si substrate we use the H_2O_2-H_2SO_4 cleaning process [2.4] before the thermal oxidation. For the production of thermal oxide on

top of the silicon wafer, a dry-wet-dry thermal oxidation processure is used at 1100°C.

For InP and GaAs the cleaning method which can remove native oxide is used for thickness and refractive index measurement experiments. As we will see in Chapter 4, the native oxide on compound semiconductors influences greatly the measurement accuracy, when the substrate with native oxide is used as standard reference.

The SiO_2 solution and TiO_2 solutions we used contain 7% SiO_2 and 9% TiO_2 and were obtained from a commercial source (Liquicoat [2.5]). They are stored in the dark in a refrigerator at about 10°C. Before using the solutions, they should be warmed to room temperature by allowing them to stand. The solutions must be mixed immediately before their use. Water introduced by an impure solvent or by air during improper mixing will deteriorate the solution causing precipitation. The more the TiO_2 is doped, the greater is the tendency to precipite. Usually ,well sealed, carefully mixed solutions are stable for several days after mixing.

In our studies we have used indium and phosphorous oxides, and Coumarin as dopants. The In_2O_3 is introduced to the solution as a

chloride or a nitrate with methanol as solvent, while the P_2O_5 is introduced as phosphate, with either methanol or propanol as the solvent. All containers we used are cleaned and dried before use with the mild detergent procedure we described for glass substrate. We carry out the film deposition in clean rooms where working surfaces are controled to class 100 conditions to avoid dust particles in the spin-on film. After mixing, we apply these solutions to the cleaned substrate surface and spin on the films at 2000-8000 RPM. For most reproducible results, extra care should be taken to use a constant volume of solution and to wet the surface completely from the center of the substrate. The time spent to wet the surface should be also constant. We noticed that the immediate environment of the spinner is also important. Before using, we clean the working area with the iso-propanol solutions. The heat treatment of coated substrate is carried out in two steps as shown in Fig.2.1 :

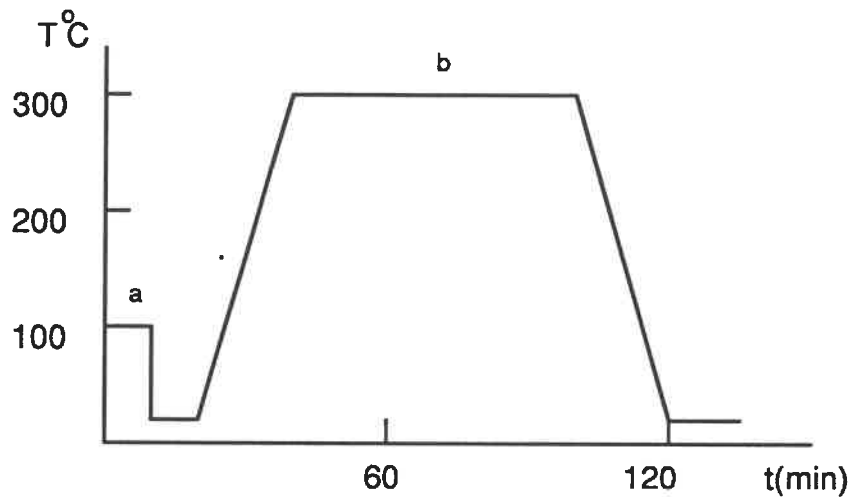

Fig.2-1 The heat treatment of the solution deposited films, showing the temperature time cycle.

First the residual solvent is driven off at 110°C for 10 min (region a). The films are then baked at a temperature between 200 and 800°C (region b) to produce hard films resistant to the original solvent and water. After the heat treatment, the film thickness and refractive index are measured with a Leitz spectrophotometer using the reflectance minimum method as we have developed in Chapter 3.

As we shall see in Chapter 5 , the film is mechanically and optically uniform to within 1.2% in the planar and 5% in vertical directions. We have also used this technique to obtain multilayers

for antireflection coating. However, for crack free films great care and complete cycling of each layer is necessary [2.6].

CHAPTER 3

DETERMINATION OF THE FILM THICKNESS AND ITS INDEX OF REFRACTION

In this chapter, we first discuss the use of normalised reflectance methods for thickness and refractive index measurements suitable for the characterisation of solution deposited thin films on silicon and glass substrates. We then introduce a general simulation method we have developed based on normalised reflectance calculations for multilayer films on transparent or absorbing substrates.

3.1 DETERMINATION OF REFRACTIVE INDEX AND THICKNESS OF SOLUTION DEPOSITED SiO_2/TiO_2 FILMS ON SILICON

The reflectance R, of a transparent film, f, of index of refraction n_f, on an absorbing substrate, s, of index of refraction n_s, and extinction coefficient k_s is [3.5,3.3]:

$$R=[r_{af}^2+p_{fs}^2+2r_{af}p_{fs}\cos(\phi_{fs}+2\beta)]/[1+r_{af}^2p_{fs}^2+2r_{af}p_{fs}\cos(\phi_{fs}+2\beta)] \quad (3.1)$$

where, for normal incidence, the reflectance at the ambient-film interface, r_{af}, is:

$$r_{af}^2=[(n_f-n_a)/(n_f+n_a)]^2 \quad (3.2)$$

and where n_a is the index of refraction of the ambient atmosphere (for air $n_a \sim 1$).

The reflectance at the film-substrate interface, p_{fs}, is:

$$p_{fs}^2=[(n_s-n_f)^2+k_s^2]/[(n_s+n_f)^2+k_s^2] \quad (3.3)$$

and ϕ_{fs} expresses by how much the phase change at the film-subtrate interface differs from π:

$$\phi_{fs}=\tan^{-1}[2k_sn_f/(n_s^2+k_s^2-n_f^2)] \quad (3.4)$$

One often defines an angle β pertaining to the constructive

interference of the film:

$$\beta=2\pi n_f d/\lambda \tag{3.5}$$

where d is the thickness of the film, λ is the incident light's wavelength.

Similarly, the reflectance at the ambient-substrate interface R_0, is:

$$R_0=[(n_s-n_a)^2+k_s^2]/[(n_s+n_a)^2+k_s^2] \tag{3.6}$$

We define the normalised reflectance of the thin film, R_{norm}, as:

$$R_{norm}=R/R_0 \tag{3.7}$$

It is R_{norm} which is always measured practically for thin films. To appreciate the effect of the constructive interference term which depends on film thickness, d, on the normalised reflectance, we show, in Fig. 3.1, the results for SiO_2 (n_f=1.42) on Si for R_{norm}

versus d at λ=400 and 600 nm.

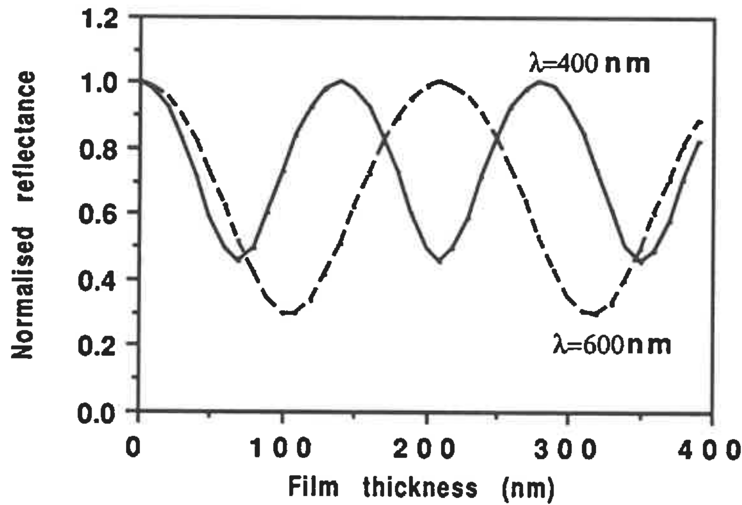

Fig.3.1 Normalised reflectance of a thin SiO_2 film with n_f =1.42 on a thick silicon substrate at a wavelength of 400 and 600 nm.

When the cosine term in equation (3.1) equals 1, there must be maxima in R, and R_{norm}=1. Similarly, when the cosine term equals -1, there must be minima for both R and R_{norm}. In particular, for the reflectance, R, these maximal and minimal values are given by the expressions:

$$R_{max}=(p+r)^2/(1+pr)^2 \qquad (3.8a)$$

$$R_{min}=(p-r)^2/(1-pr)^2 \qquad (3.8b)$$

where, for simplicity, we have eliminated the subscripts a, f and s of p and r.

If we neglect the substrate absorption (k_s=0) the equations (3.8) become:

$$R_{max}=(n_s-1)^2/(n_s+1)^2 \qquad (3.9a)$$

$$R_{min}=(n_a n_s-n_f^2)^2/(n_a n_s+n_f^2)^2 \qquad (3.9b)$$

Expressions (3.8b) and (3.9b) can easily be used to determine the thin film refractive index on a reflective surface such as silicon, since, at the d-λ combination which leads to the expression (3.8b), the film refractive index n_f is only a function of n_s, k_s, and R_{min}. Similarly, for the substrate at any given wavelength, R_o is solely determined by n_s and n_k. Therefore, we can conclude from equation (3.7) that n_f is uniquely determined by n_s, k_s, and $R_{norm,minimum}$ (that is the substrate's optical parameters and the measured $R_{norm,minimum}$

value).

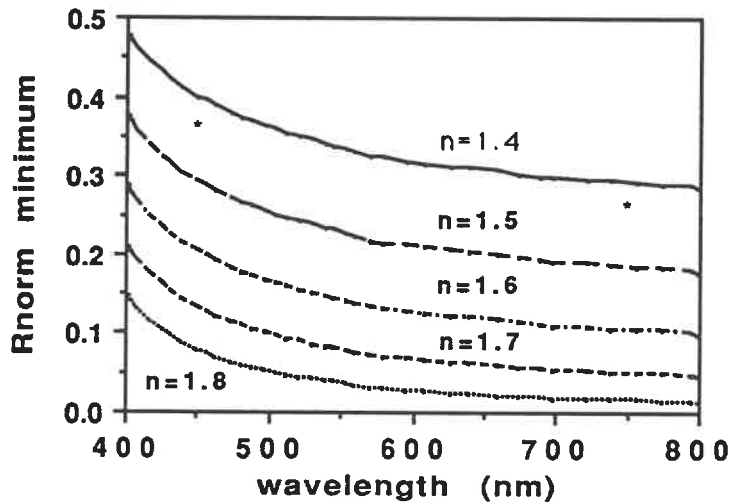

Fig.3.2 Normalised reflectance minimum and wavelength relations for films of different refractive index ranging from 1.40 to 1.80 on a silicon substrate.

Fig.3.2 shows a family of $R_{norm,minimum}$-λ curves constructed with the use of expression (3.8b). To determine the refractive index of the film n_f, in practice, we first determine the $R_{norm,minimum}$ and its corresponding wavelength values in the experimental R_{norm}-λ curve of the film (such as Fig.3.3 below). Then we can find the refractive index of the film through interpolation using Fig.3.2.

We illustrate this procedure with a numerical example. Fig.3.3 shows a simulated R_{norm}-λ curve of a transparent film of 400 nm thickness with a refractive index of 1.42 on a silicon substrate, in the wavelength range from 400 to 800 nm.

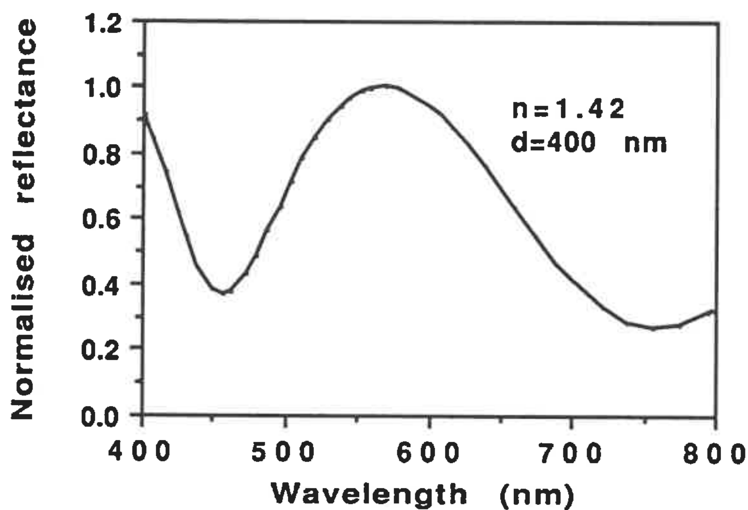

Fig.3.3 The R_{norm}-λ curve of a transparent film 400 nm thick with a refractive index of 1.42.

We see that in this wavelength range there are a pair of minima at 456 nm (R_{norm}=0.371) and 756 nm (R_{norm}=0.267). Consulting Fig.3.2 or Appendix 2 we see that this pair corresponds to a unique value of n=1.42. The accuracy of the technique is limited only by the graphical or numerical resolution employed. With n_f

known at the wavelength position where a normalised reflectance minimum appears, we can use equation (3.1) to find d at this wavelength. It must be noted that for equation (3.1) the solution for d is multivalued, because various combinations of λ-d can generate the same R or R_{norm} values (Fig.3.1). To correctly solve for d, two methods can be used. The first method uses two R_{norm} readings at wavelengths λ_1 and λ_2 and then consults the calculated $R_{norm}(\lambda_1)$-$R_{norm}(\lambda_2)$ curve for various d values such as in Fig.3.4. The wavelengths λ_1 and λ_2 are arbitrarily selected in a wavelength range from 400 nm to 800 nm [3.4]. The second method is useful for thicker films with two or more than two minima in its normalised reflectance spectrum [3.9]. The film thickness can be expressed as:

$$d = \frac{\lambda_1 \lambda_2}{2(n_f^2 - \sin^2\theta)^{\frac{1}{2}}(\lambda_1 - \lambda_2)} \left(1 - \frac{\Phi_{fs1} - \Phi_{fs2}}{2\pi}\right) \tag{3.10}$$

where, λ_1 and λ_2 denote the extrapolated values of two adjacent minima, and Φ_{fs1} and Φ_{fs2} refer to the phase shift at the film-substrate interface at these two wavelengths λ_1 and λ_2, respectively, which can be calculated by equation (3.4). The term $[1 - (\Phi_{fs1} - \Phi_{fs1})/2\pi]$ is the correction factor, and it depends upon the

optical properties of the substrate.

After we get a thickness value from one of the two methods, we can use equation (3.1) to get a more accurate value.

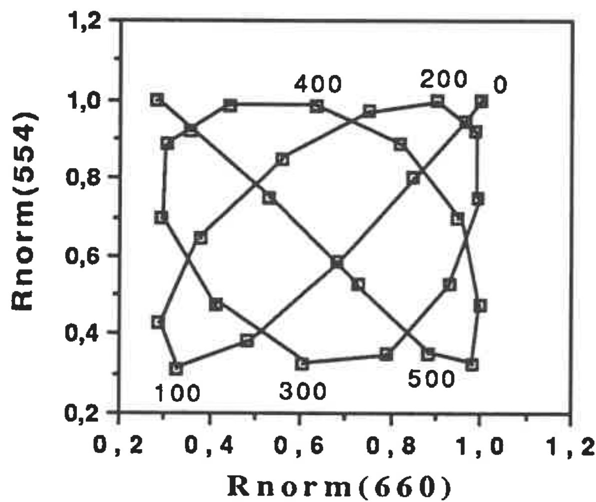

Fig.3-4 R_{norm}(554 nm)-R_{norm}(660 nm) at different film thicknesses for a film of n_f=1.42 on silicon substrate.

To determine the refractive index and the thickness of transparent thin films on SiO_2 and glass, the characteristic matrix method [3.6] [3.7] can be used. We analyse an air-transparent film-transparent substrate assembly with a light beam of wavelength λ incident on the film with an angle of incidence ϑ (Fig.3.5).

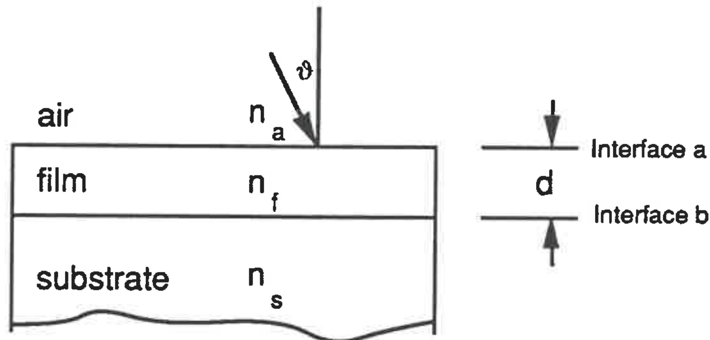

Fig.3-5 Air, film, substrate assembly. The film thickness is d. The refractive indices are n_a ,n_f ,n_s for air, the film and the substrate. The substrate is semi-infinite.

The characteristic matrix of the j'th film expresses a linear relationship between the field E_a, H_a on top of the j'th film to the field E_b, H_b on its emergent side:

$$\begin{bmatrix} E_a \\ H_a \end{bmatrix} = \begin{bmatrix} \cos\delta_j & \frac{i \sin\delta_j}{\eta_j} \\ i\,\eta_j \sin\delta_j & \cos\delta_j \end{bmatrix} \begin{bmatrix} E_b \\ H_b \end{bmatrix} \tag{3.11a}$$

or,

$$[E_a]\begin{bmatrix} 1 \\ Y_a \end{bmatrix} = \begin{bmatrix} \cos\delta_j & \frac{i \sin\delta_j}{\eta_j} \\ i\,\eta_j \sin\delta_j & \cos\delta_j \end{bmatrix} \begin{bmatrix} 1 \\ Y_b \end{bmatrix}[E_b] \tag{3.11b}$$

where,

$$\delta_j = 2\pi\eta_j d_j \cos\vartheta_j/\lambda \tag{3.12}$$

denotes the phase retardation, and η_j is the optical admittance which is valid for any angle of incidence: $\eta = n\cos\vartheta$, for TE waves (or S-waves, where E is parallel to the boundary and H tilted at angle ϑ), $\eta = n/\cos\vartheta$, for TM waves (or P-waves, where H is parallel to the boundary and E tilted at angle ϑ).

Here,

$$\begin{bmatrix} \cos\delta_j & \dfrac{i\sin\delta_j}{\eta_j} \\ i\,\eta_j\sin\delta_j & \cos\delta_j \end{bmatrix}$$

is called the characteristic matrix of the film.

We define:

$$\begin{bmatrix} \cos\delta_j & \dfrac{i\sin\delta_j}{\eta_j} \\ i\,\eta_j\sin\delta_j & \cos\delta_j \end{bmatrix} \begin{bmatrix} 1 \\ \eta_s \end{bmatrix} = \begin{bmatrix} B \\ C \end{bmatrix} \tag{3.13}$$

as the characteristic matrix of the film stack when the emerging side of the j'th film layer is another thin film, or as the characteristic matrix of the film-substrate combination when the emergent side of the j'th film is a semi-infinitive thick substrate.

Y=C/B is called the admittance of the film stack or film-substrate assembly.

$$Y=C/B$$

$$=(\eta_s\cos\delta_f+i\eta_f\sin\delta_f)/(\cos\delta_f+i(\cos\delta_f+i(\eta_s/\eta_f)\sin\delta_f)$$

(3.14)

From (3.10) to (3.14) we get:

$$r=\{(\eta_a-\eta_s)\cos\delta_f+i[(\eta_a\eta_s/\eta_f)-\eta_f]\sin\delta_f\}/$$

$$\{(\eta_a+\eta_s)\cos\delta_f+i[(\eta_a\eta_s/\eta_f)+\eta_f]\sin\delta_f\}$$

(3.15)

The power reflectance is:

$$R=r\ r^*$$

$$=\{(\eta_a-\eta_s)^2\cos^2\delta_f+i[(\eta_a\eta_s/\eta_f)-\eta_f]^2\sin^2\delta_f\}/$$

$$\{(\eta_a+\eta_s)^2\cos^2\delta_f+i[(\eta_a\eta_s/\eta_f)+\eta_f]^2\sin^2\delta_f\}$$

(3.16)

where, r^* is the complex conjugate of r.

At normal incidence ($\theta=0$),

$$R=\{(n_a-n_s)^2\cos^2\delta_f+[n_an_s/n_f-n_f]^2\sin^2\delta_f\}/$$

$$\{(n_a+n_s)^2\cos^2\delta_f+[n_an_s/n_f+n_f]^2\sin^2\delta_f\}$$

(3.17a)

and,

$$\delta_f=2\pi n_f d_f/\lambda \qquad (3.17b)$$

When the reflectance of an air-film-substrate assembly R is normalised to the reflectance of an air-substrate assembly R_o we get:

$$R_{norm}=R/R_o \qquad (3.18)$$

where,

$$R_o=(n_a-n_s)^2/(n_a+n_s)^2 \qquad (3.19)$$

If we fix the wavelength at any nominal value λ_o and vary the n_fd_f product, R and R_{norm} go through maxima and minima at n_fd_f = 1/4 λ, 2/4 λ, 3/4 λ ...... m/4 λ for integer values of m.

Fig.3.6 provides a numerical example of this variation for R_{norm} vs. n_fd_f with n_a=1, n_s=1.5. From this figure we can see that when $n_f>n_s$,

$R_{norm} \geq 1$, when $n_f < n_s$, $R_{norm} \leq 1$.

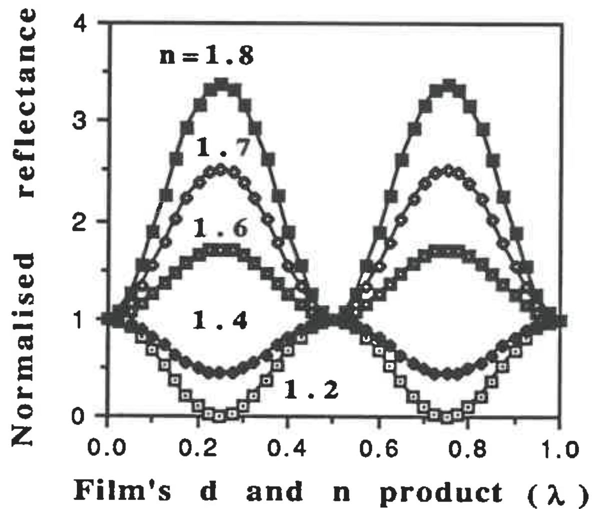

Fig.3.6 R_{norm}-$d_f n_f$ relations for films with different refractive index.

Of course in practical applications, the film thickness is fixed by deposition and we sweep the wavelength of the incident light to get reflectance or normalised reflectance spectra.

An example of this types of curves is in Fig.3.7 which gives the normalised reflectance and wavelength spectra for a series of three film thicknesses with the refractive index of $n_f = 1.7$.

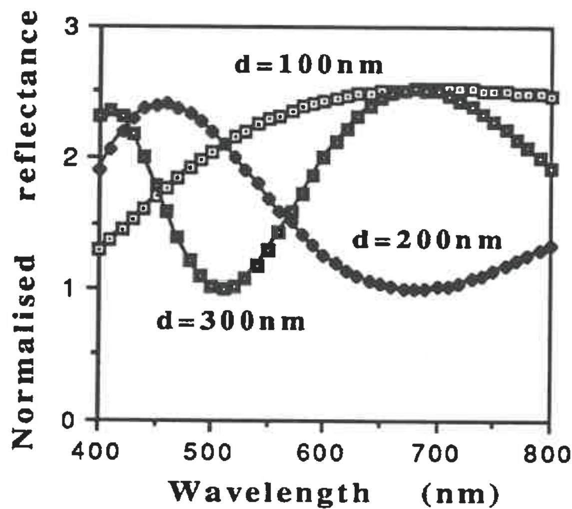

Fig.3.7 Example, normalised reflectance for films of different thickness of 100, 200 and 300 nm and index of refraction n_f=1.7 on glass (n_s=1.52 at 633 nm).

For a given film-substrate, it is not difficult to deduce from measured normalised reflectance spectra at the same time the film thickness and refractive index, when the film is thick enough to generate at least one minimum (when $n_a<n_s$) or maximum (when $n_a >n_s$). If the film is very thick, there will be several maxima or minima, and we can get a more accurate refractive index value for the films, and indeed obtain $n(\lambda)$ at wavelengths corresponding to

these extrema.

Fig.3.8 gives the values of reflectance minima (or maxima) as a function of wavelength for a glass substrate for a range of film refractive indices. When the refractive index of the film is known, we can deduce the film thickness from R_{norm} readings at two wavelengths as in the case for films on silicon. If ambiguity exists, we must use the reading at a third wavelength.

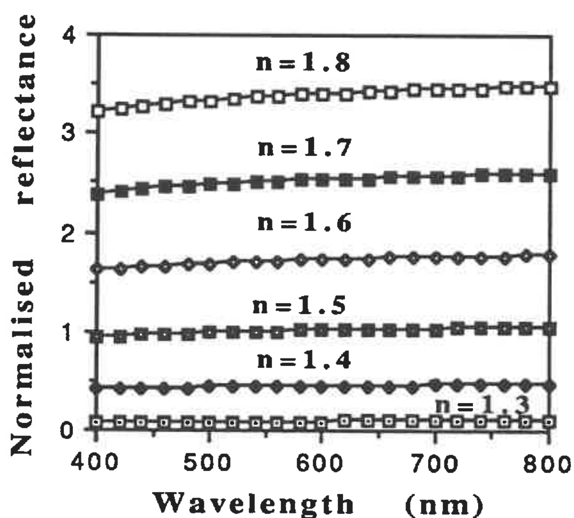

Fig.3.8 The $R_{norm,minimum}$ or $R_{norm,maximum}$ and wavelength relations for various film refractive index values on glass.

For multi-layer films on transparent substrates, we can get the reflectance or normalised reflectance with the use of the characteristic matrix of each film. The characteristic matrix of an assembly of M layers, each with admittance η_j and angle δ_j is:

$$\begin{bmatrix} B \\ C \end{bmatrix} = \prod_{j=1}^{M} \begin{bmatrix} \cos\delta_j & \frac{i \sin\delta_j}{\eta_j} \\ i\,\eta_j \sin\delta_j & \cos\delta_j \end{bmatrix} \begin{bmatrix} 1 \\ \eta_s \end{bmatrix}$$

(3.20)

Through successive use of expressions (3.11)-(3.19), we can calculate the power reflectance R for the air-multilayer-substrate assembly. If we know the thickness and optical parameters of each of the other film layers, the thickness d of the top layer can be deduced from the R_{norm}-wavelength curve of the whole assembly.

For practical laboratory measurement conditions we often must take into account the fact that the rear substrate surface also will reflect light. Fortunately, for an air-film-substrate assembly, when the substrate thickness is in the range of about 0.4-1 mm, as is usually used for the glass integrated optics , generally there will be no interference between the two surfaces. In Fig.3.9 we modify

Fig.3.5 to allow for reflection at the back surface with reflectance R_o and define R' to be the total reflectance and T' the total transmission of the overall film-substrate. We can express R' and T' in terms of the above reflection:

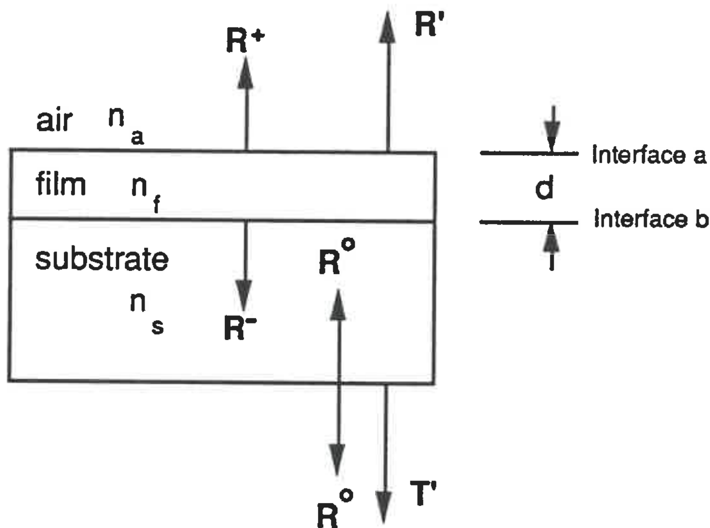

Fig.3.9 Practical air-films-substrate-air assembly.

$$R'=R+(1-R)^2R_0+(1-R)^2R_0^2R+(1-R)_2R_0^3R^2+....$$

$$= R+(1-R)^2[R_0/(1-R_0R)]$$

(3.21)

$$T'=(1-R)(1-R_0)(1+RR_0+R^2R_0^2+......)$$

$$=(1-R)(1-R_0)[1/(1-RR_0)].$$

(3.22)

and

$$T'+R'=1$$

(3.23)

The reflections from the film to the air at interface a (R+), and from the film to the substrate at interface b (R-), are the same for non-absorbing films, and we denote them both as R_0 [3.6].

We note that when there is no film on the substrate, T' and R' become:

$$R'_0=R_0+R_0(1-R_0)/(1+R_0)$$

(3.24)

$$T'_0=(1-R_0)/(1+R_0)$$

and (3.25)

$$T'_0+R'_0=1$$

(3.26)

Finally, to make contact with the measurement approach, the reflectance of the whole air-films-substrate-air assembly can be normalised with the reflectance of the air-substrate-air assembly.

As a numerical example of the normalised reflectance we calculate R_{norm} and R'_{norm} for a semi-infinitive SiO_2 substrate, and a film with n=1.70 and d=300 nm. The result is shown on Fig.3.10 as well as the ratio of R'/R and R'_0/R_0.

Since

$$R'_{norm}=R_{norm}(R'/R)/(R'_0/R_0)$$

$$=R_{norm}[(1+R_0)/2]\{1+[(1-R)\ \ 2(R_0/(1-RR_0))]\}/R$$

(3.27)

We see that the R'_{norm} function has the same peak and valley structure as R_{norm}. From Fig.3.10 we observe that compared with R_{norm}, the R'_{norm} value is smaller (about 1/2 in fact). For the normalised reflectance measurement, the effect of reflection at the rear surface is to lower (about 50%) the value of the normalised reflectance at all wavelengths, but especially near the R_{norm} maxima. In our technique we measure directly the reflectance of the substrate including back surface reflection. This removes the necessity to either make completely absorbing or scattering the

back surface for reliable measurements as is practiced almost everywhere, and in the method of use suggested by Leitz for their MSVP instrument.

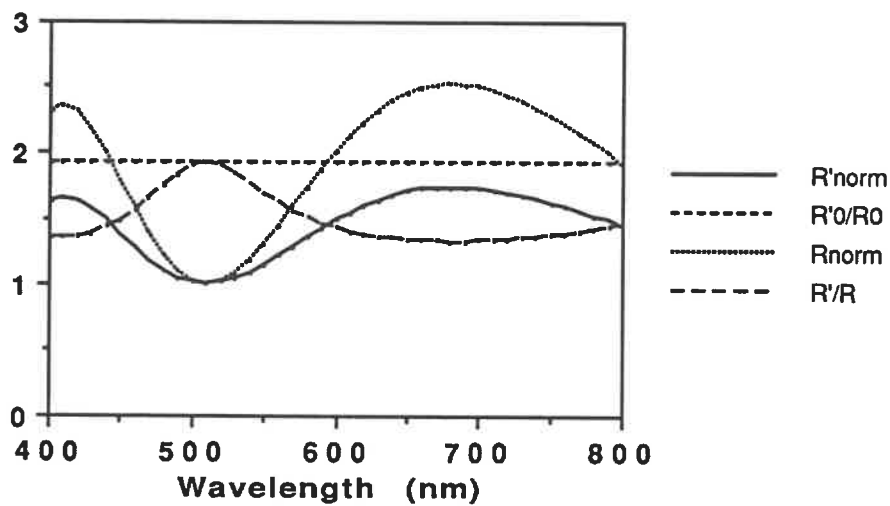

Fig.3.10 R'_{norm}, R_{norm} and R'/R, R'_0/R_0-λ curves of a transparent film with n=1.7 and d=300 nm on glass substrate.

3.2 NORMALISED REFLECTANCE OF ABSORBING FILMS ON ABSORBING OR TRANSPARENT SUBSTRATES

In the preceeding paragraph the normalised reflectance of transparent films on silicon and on glass are discussed. Often pure or transparent films such as SiO_2 are used in combination with optically absorbing films or thin metal films to obtain special effects. In such cases we must have a general method to simulate the optical characteristics and to analyse the optical parameters of such a multilayer thin film system. In this paragraph we shall develop a simple calculation method based on general principles which can at same time be used for absorbing or non-absorbing films and substrates.

To calculate the normalised reflectance of absorbing films on absorbing substrates, the characteristic matrix method can be used, as in the case of transparent films on transparent substrate. However, this time, both the refractive indices of the substrate and of the films are both complex numbers. For convenience of calculation, and in conformity with the practical normalised reflectance measurement, we adopt a notation system which assigns

the subscript according to the natural film deposition order and uses s and a for the substrate and ambient, respectively.

At normal incidence, $\vartheta=0$, the characteristic matrix of the j'th film layer is:

$$\begin{bmatrix} \cos\delta_j & \frac{i \sin\delta_j}{n_j} \\ i\, n_j \sin\delta_j & \cos\delta_j \end{bmatrix}$$

(3.28)

where

$$\delta_j=2\pi n_j d/\lambda.$$

The characteristic matrix of the multifilms-substrate combination is:

$$\begin{bmatrix} B \\ C \end{bmatrix} = \begin{bmatrix} \cos\delta_j & \frac{i \sin\delta_j}{n_j} \\ i\, n_j \sin\delta_j & \cos\delta_j \end{bmatrix} \begin{bmatrix} \cos\delta_{j-1} & \frac{i \sin\delta_{j-1}}{n_{j-1}} \\ i\, n_{j-1} \sin\delta_{j-1} & \cos\delta_{j-1} \end{bmatrix} \cdots \begin{bmatrix} \cos\delta_1 & \frac{i \sin\delta_1}{n_1} \\ i\, n_1 \sin\delta_1 & \cos\delta_1 \end{bmatrix} \begin{bmatrix} 1 \\ n_s \end{bmatrix}$$

(3.29)

In practice we calculate this product of matrices from bottom to top. Performing the first multiplication of the matrix of the first layer gives an admittance of the substrate-film #1 combination y_1:

$$\mathcal{Y}_1=(\mathcal{Y}_s\cos\delta_1+in_1\sin\delta_1)/(\cos\delta_1+(i\ \mathcal{Y}_s/n_1\sin\delta_1))$$

$$=y_1+i\ Y_1 \qquad (3.30)$$

where

$$\mathcal{Y}_s=n_s+i\ k_s.$$

This process can be continued until the j'th layer as:

$$\mathcal{Y}_j=(\mathcal{Y}_{j-1}\cos\delta_j+i\ n_j\sin\delta_j)/(\cos\delta_j+(i\ y_{j-1}/n_j\sin\delta_j))$$

$$= y_j+i\ Y_j \qquad (3.31)$$

The amplitude reflectivity of the j'th layer and underlying film substrate combination is:

$$r_j=(n_a-\mathcal{Y}_j)/(n_a+\mathcal{Y}_j)$$

$$=((n_a-y_j)-i\ Y_j))/((n_a+y_j)+i\ Y_j)) \qquad (3.32)$$

The reflectance of the films substrate assembly up to the j'th layer is:

$$R_j=((n_a-y_j)^2+Y_j^2)/((n_a+y_j)^2+Y_j^2) \qquad (3.33)$$

The expression of the real and imaginary part of $\mathcal{Y}_1$, y_j and Y_j,

can be obtained as follows.

First,

$$\delta_j=(n_j-i\ k_j)(d2\pi/\lambda)=\delta_{1j}-i\ \delta_{2j} \tag{3.34}$$

where

$$\delta_{1j}=n_jd_j2\pi/\lambda,$$

and

$$\delta_{2j}=\ k_jd_j2\pi/\lambda.$$

Thus

$$\cos\delta_j=(e^{i\delta_j}+e^{-i\delta_j})/2=\cos\delta_{1j}\cosh\delta_{2j}+i\ \sin\delta_{1j}\sinh\delta_{2j},$$

$$=c_{1j}+i\ c_{2j} \tag{3.35}$$

where

$$c_{1j}=\cos\delta_{1j}\cosh\delta_{2j},$$

and

$$c_{2j}=\sin\delta_{1j}\sinh\delta_{2j}.$$

Similarly we have:

$$\sin\delta_j=s_{1j}+i\ s_{2j} \tag{3.36}$$

where

$$s_{1j}=\sin\delta_{1j}\cosh\delta_{2j}.$$

and

$$s_{2j}=-(\cos\delta_{1j}\sinh\delta_{2j}).$$

After some mathematical manipulation we can get formulas for the admittance of the film-substrate combination up to layer j with which we can carry out all the reflectance calculations in the range of real numbers:

$$y_j=(a_{1j}a_{3j} + a_{2j}a_{4j}) \;/\; (a_{3j}{}^2 a_{4j}{}^2), \tag{3.37}$$

$$Y_j=(a_{2j}a_{3j} - a_{1j}a_{4j}) \;/\; (a_{3j}{}^2 a_{4j}{}^2), \tag{3.38}$$

where

$$a_{1j}=y_{j-1}c_{1j} - Y_{j-1}c_{2j} + k_j s_{1j} - n_j s_{2j},$$

$$a_{2j}=Y_{j-1}c_{1j} + y_{j-1}c_{2j} + n_j s_{1j} + k_j s_{2j},$$

$$a_{3j}=c_{1j}-q_{1j},$$

$$a_{4j}=c_{2j}-q_{2j},$$

(3.39)

and

$$q_{1j}=(n_jb_{1j}-k_jb_{2j}) \ / \ (n_j^2+k_j^2),$$

$$q_{2j}=(k_jb_{1j}+n_jb_{2j}) \ / \ (n_j^2+k_j^2),$$

(3.40)

where,

$$b_{1j}=Y_{j-1}s_{1j} + y_{j-1}s_{2j},$$

$$b_{2j}=Y_{j-1}s_{2j} - y_{j-1}s_{1j}.$$

(3.41)

The normalised reflectance of the whole M-layer system is

$$R_{norm}= R/R_0.$$

(3.40)

where

$$R_0=((n_s-n_a)^2+k_s^2)/((n_s+n_a)^2+k_s^2.$$

(3.41)

and R can be calculated according to (3.31).

For absorbing films on a transparent substrate one must take

the rear surface into account [3-6]. Now, the reflectance of the light from the ambiant Ra+ are not simply the same as the reflectance of the light from substrate Ra- due to the film absorption. The total reflectance of the whole system, taking this into account, is:

$$R= R_a{}^{+}+(T_a{}^{+}T_a R_b{}^{+}) / (1-R_a{}^{-}R_b{}^{+}), \tag{3.44}$$

with

$$T=(1-R)\sum_{j=1}^{M} \psi_j \tag{3.45}$$

and

$$\Psi_j= y_{j-1} / [y_j(a_{3j}{}^2+a_{4j}{}^2)]. \tag{3.46}$$

Here Ψ_j is the ratio of the optical power density between two adjacent interfaces, j and j-1 [3.7,3.2]. For practical measurement and simulation in the case of transparent substrates, normalisation is carried out with a bare substrate as reference, and it is assumed that the rear suface is flat and without any film on it. Note that when the film is thin or when the k value of the film is not large,

the rear suface will have the effect of lowering the reflectance value. When the film is very thick, the reflectance of the whole system will not be influenced by the rear suface, and the simple one surface approach can be used.

We have tested the formulas developed in this section both by experiment and by comparision with the published results for thin films on absorbing and transparent substrates. Both single layer [3.1][3.7] or multi-layer [3.7] expressions were tested and found to be correct. In the following chapters we use these formulas to simulate various thin film and substrate assemblies. As an example, one set of formulas used to calculate the normalised reflectance of eight transparent films on silicon substrate is listed at Appendix 3 of this thesis.

3.3 EXPERIMENTAL USE OF THE NORMALISED REFLECTANCE METHOD

To verify our formulas and methods using the normalised reflectance method, two samples of wet thermal oxide films of differing thickness (which turned out to be 857.5 nm and 762 nm thick) were grown at 1100 ^{o}C on silicon wafers and the normalised reflectance of the film-substrate combination was measured [3.4] [3.11]. The 857.5 nm thick film generated three reflectance minima between 400 and 800 nm. From these minima we found the refractive index of the film at particular wavelengths using Fig.3.2. We found that at these wavelengths, the refractive index data agrees well with that of the pure bulk SiO_2 refractive index curve reported in the literature [3.9] as Fig.3.11 shows. Using these index of refraction values we then employed the results of the normalised reflectance calculation for this film-substrate assembly to calculate the film thickness and found it to be 857.5 nm.

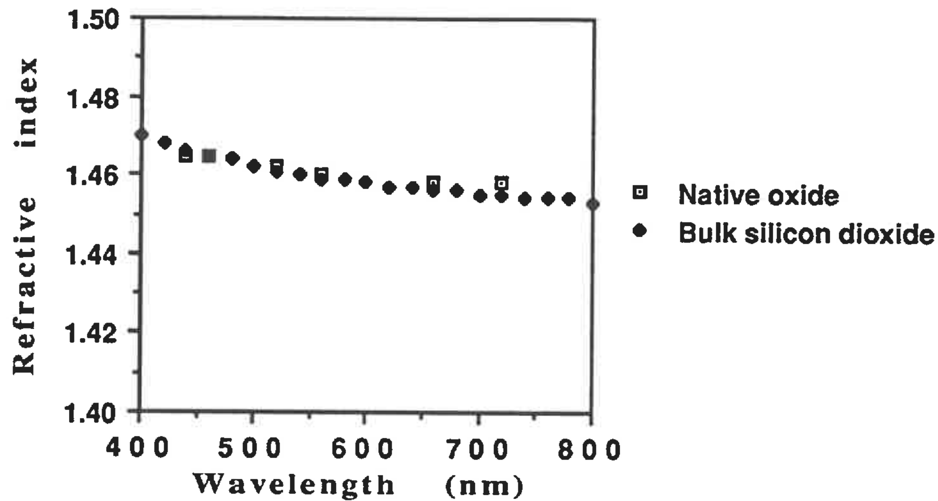

Fig.3.11 Refractive index of the thermaly grown SiO_2 on silicon.

As a check on this procedure we used these refractive index and thickness results to simulate the normalised reflectance of the film substrate combination in the wavelength range from 400 to 800 nm. Fig.3.12 shows the results of the simulation calculation compared with the measured normalised reflectance of the film-substrate combination. The two curves agree to within 2.5 %.

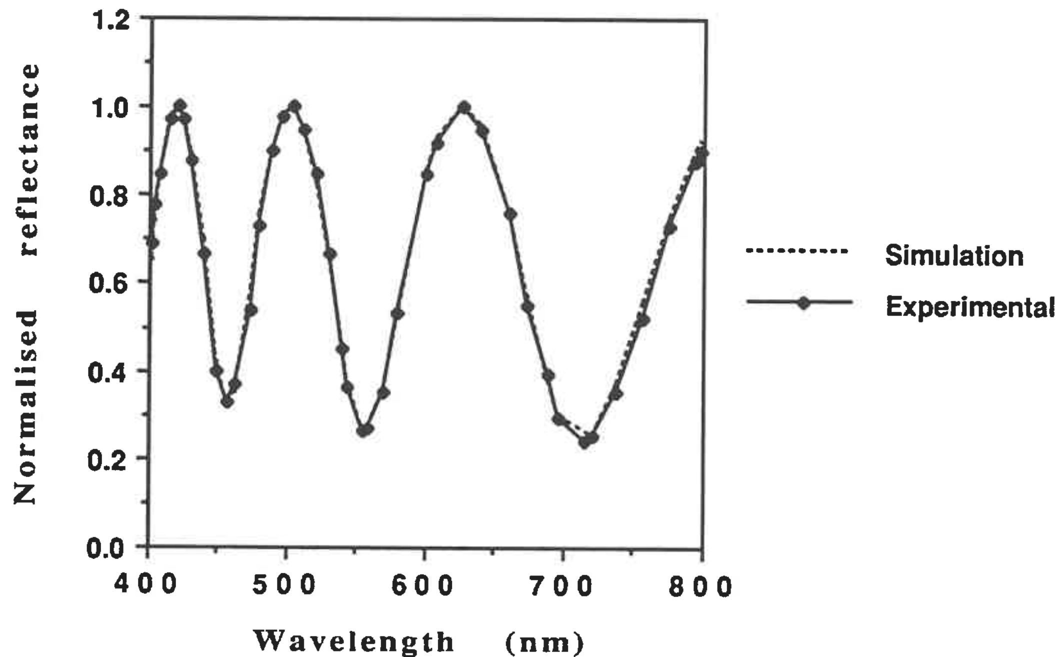

Fig.3.12 Simulated and experimental normalised reflectance of thermally grown SiO_2 of 857.5 nm on silicon.

This experiment shows that the reflectance minimum method can well suit our purpose of the refractive index and the thickness mesurement on silicon surfaces. For solution deposited thin films, similar dispersion curves can be obtained which is useful in thin film design and simulation as we will show in Chapter 4. Other examples will be shown in Chapter 5 and Chapter 6. In Chapter 6 the

results from the normalised reflectance method are compared with the waveguide effective refractive index method.

As for the thin films on glass substrates, from Fig.3.6 and Fig.3.7 it is found that when a refractive index difference of 0.05 or great between film and substrate exists, it is not difficult to measure the film thickness and refractive index by refractive maximum method. For a 50% TiO_2 doped SiO_2 film on glass substrate, the normalised reflectance maximum is about 2.6 when the substrate is semi-infinitively thick and about 1.75 when the substrate is two sided. The refractive index difference detectability of this method is determined by the signal/noise ratio of the equipment used. The Leitz spectrophotometer we used gives a refractive index difference limit of about 0.01 for the glass substrate. Examples for the normalised reflectance of thin films on glass will be shown in Chapter 6.

CHAPTER 4

SOLUTION DEPOSITED SiO_2 ON Si, GaAs AND InP

Thin dielectric films on semiconductor substrates are used in various ways. For optoelectronics and integrated optics applications as we discussed in Chapter 1 and Chapter 2, in addition to good electrical and mechanical properties, a film both easy to prepare and convenient to control is useful. Among the parameters one needs to control in a broad range are the index of refraction and the film thickness uniformity. Also, some facility to introduce other optically active ions is important.

For thin films of less than 0.5 μm thick, a single application of alkoxide of silicon is enough to produce a very smooth layer of SiO_2 with index of refraction in the range of 1.4 to 1.45 according to the processing condition, as the results in Chapter 2 show. For films with higher refractive index, titanium alkoxide can be added to control the index of refraction.

In this chapter the details of preparation of solution deposited SiO_2 on semiconductors are discussed. The genaral analysis method

developed in Chapter 3 is used. As to the application of solution deposited silicon dioxides on semiconductor surfaces, we refer the reader to Chapter 6.

The results of Chapter 2 and reference [4.6] [4.2] show that depending on the amount of titanium added and on the processing conditions, the introduction of titanium alkoxide can change the refractive index of the final films. But the films also show some tendency of cracking which is generally attributed to the moderate temperature of the process (300-500°C) when titanium content surpasses 50% and when the film thickness for one application is greater than 150 nm [4.3]. The spin-on method is used to suit the needs of microelectronic processing.

We used commercially available E.Merck liquicoat solutions [4.4] containing 7% and 9% SiO_2 and TiO_2 respectively. The substrate we used are P-doped [100] Si, n-type [100] InP. Before application of the solution, the substrate is cleaned using the standard solvent and de-ionized water process as we discussed in Chapter 2. For the InP substrate, we use the H_2SO_4:H_2O_2:H_2O (4:1:1) solution to remove the native oxide on the substrate, and we then rinsed the substrate in de-ionized water and then dried it by nitrogen gas. The spin-on coating

is carried out in a 100 class cleanroom. To avoid deterioration of the coating solution in the case of codoping, the solution is mixed before coating.

The two stage temperature processing is carried out in which coated films containing the residual organic solvent are baked to evaporate the solvent and other volatile components until a hard film is formed (fig.2.1). The resulting film will resist both the original solvent and water. To produce a multilayer film without cracking, complete cycling for each application of coat is exercised to avoid the redissolving of the coating.

To determing the thickness and the refractive index of the film on semiconductor, the normalised reflectance method described in Chapter 3 is used. In this method, at normal incidence the reflectance of the specimen of a transparent film and semiconductor substrate combination R(d) is measured and compared with the reflectance of the fresh surface of the same semiconductor R(0) at wavelength range from 400 to 800 nm to get the normalised reflectance $R_{norm}(d)$:

$$R_{norm}(d) = R(d)/R(0) \qquad (4.1)$$

where d is the film thickness.

The measured normalised reflectance can be compared with the calculated value, and from the reflectance minimum we can at the same time deduce the value of refractive index and film thickness at a given wavelength as we described in Chapter 3. For silicon substrate Fig. 3.2 is used. Corresponding figures for GaAs and InP are presented in Appendix 3. The optical constants used for these calculations are listed in Appendix 2.

We began our experimental work by depositing in one process thin films on different substrate. For each film we found that the normalised reflectance measurements for the InP substrate were anomalous and could be reconciled with those of Si and GaAs by taking into account a presence of an intermediate native oxide layer which had the effect of changing the reference surface used in the normalised reflectance measurement. To make possible such measurement on InP, we began by calculating native oxides of varying thicknesses range from 5 to 30 nm and comparing these results with that of silicon. We assume the refractive indices involved to be 1.45 for SiO_2, and 1.9 for In_2O_3-P_2O_5. The results are shown in Fig. 4.1 and Fig.4.2. The overall effect of the presence of a

native oxide on InP is to increase the reflectivity compared to that of a Si substrate.

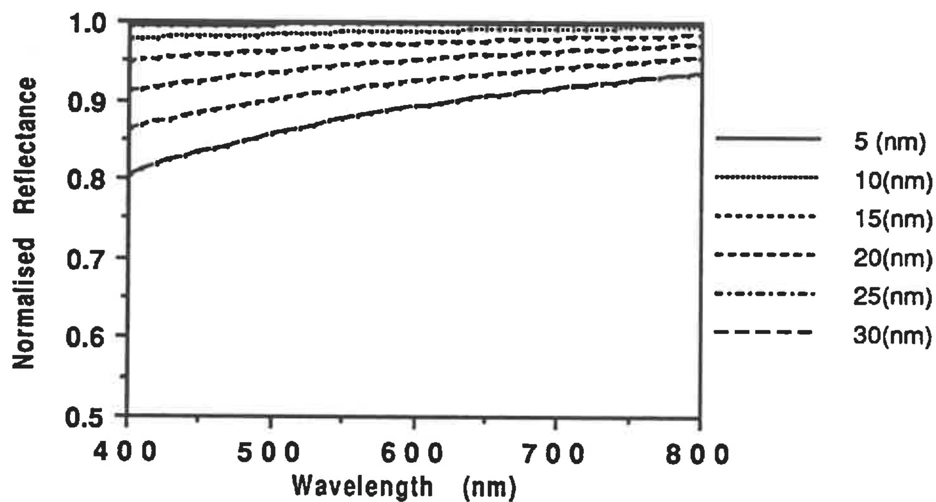

Fig.4.1 The calculated normalised reflectance spectrum of SiO_2 films with thickness ranging from 5 to 30 nm on a silicon substrate.

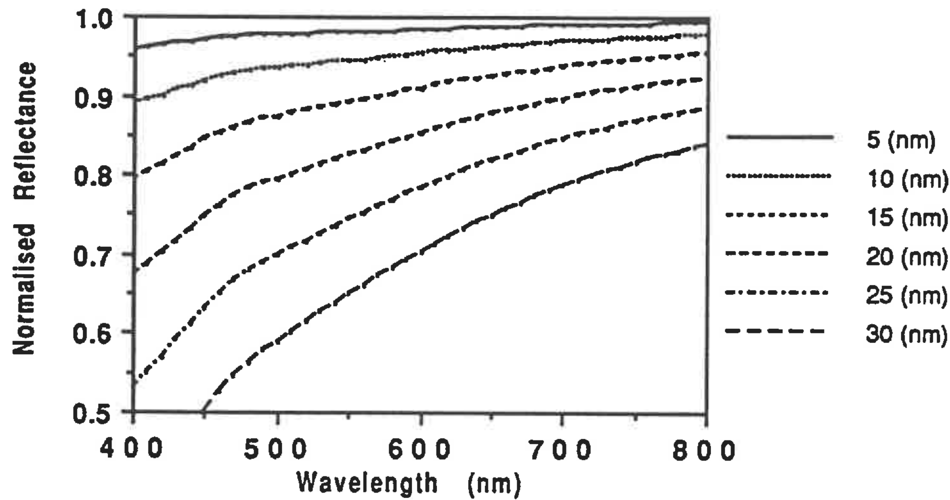

Fig.4.2 The calculated normalised reflectance spectrum of native oxide with thickness ranging from 5 to 30 nm on a InP substrate.

If we take an InP substrate with a native oxide of thickness d_1 on it to measure a film of same refractive index but with the thickness of d_2, instead of equation (4.1) we have:

$$[R_{norm}\ (d2)]_m' = R\ (d_2)/R(d_1) \tag{4.2}$$

where, according to equation (4.1):

$$R\ (d_1) = R_{norm}(d_1)^* R(0).$$

By comparing equation (4.1) and that of (4.2), it is easy to find that $[R_{norm}(d_2)]_m'$ is just the real normalised reflectance $R_{norm}(d_2)$ divided by $R_{norm}(d_1)$ which is a curve with magnitudes less than 1 (Fig.4.2). Numerical calculation shows that if we take a InP substrate with a native oxide on it as reference to measure other films on the same substrate, the values of $[R_{norm}(d_2)]_m'$ at every wavelength from 400 to 800 nm is always greater than the real value $R_{norm}(d_2)$. In the case of thicker films we will get peaks with $[R_{norm}(d_2)]_m'$ values great than 1. To get the correct thickness and refractive index value, the results must be corrected through the use of equation (4.1) and equation (4.2). Without correction, both the deduced refractive index and thickness value of the film will be smaller than their actual value.

The refractive index of the solution deposited SiO_2 films depends on the processing condition and the dopant concentration. The pure SiO_2 films on silicon exibit process related dispersion characteristics. Fig.4.3 is the refractive index of solution deposited SiO_2 obtained at different baking temperatures. Also shown in this figure is the dispersion curve of fused silica according to reference

[4.3]:

$$n_\lambda = \sqrt{c_0\frac{\lambda^2}{(\lambda^2-c_1^2)} + c_2\frac{\lambda^2}{(\lambda^2-c_3^2)} + c_4\frac{\lambda^2}{(\lambda^2-c_5^2)} + 1}$$

$$c = \begin{bmatrix} 0.6961663 \\ 0.0684043 \\ 0.4079426 \\ 0.1162414 \\ 0.8974794 \\ 9.8961610 \end{bmatrix} \qquad (4.3)$$

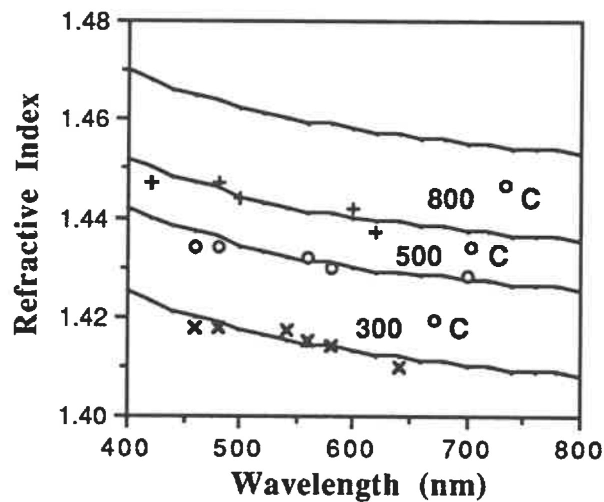

Fig.4.3 Measured refractive index of spin-on SiO_2 film deposited on Si at 300 °C (×), 500 °C (○) and 800 °C (+). The solid curves are the dispersion relation of reference [4.3].

We note the experimental curves of fig.4.3 can all be obtained from expression (4.3) by a simple shift of the index of refraction by a constant, Δn, which for the three experimental curves of 800°C, 500°C and 300°C baked solution deposited silicon dioxide are 0.018, 0.028, and 0.045 respectively. We conclude that the higher the heating temperature, the denser and more like the thermal oxide the spin-on film becomes. In case of TiO_2 doped SiO_2, the experimental results can be fitted with a linear relationship as figure 4.4 shows.

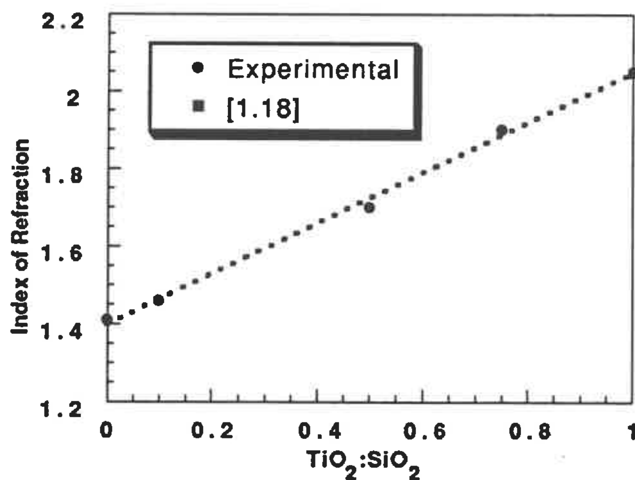

Fig.4.4 Refractive index of solution deposited SiO_2 films doped with TiO_2 and baked at 300°C.

We note that the index of refraction of pure spin-on TiO_2 (2.05+/-0.05) of reference [1.18] falls on the extrapolation of our

measured curve. If the refractive index of the dopant is known, and the same processing is carried out we can conveniently estimate the refractive index of the resulting films using this curve in thin film design and measurement [1.18].

The Ti-doped films can serve as anti-reflection coatings for semiconductor surface. With a suitable thickness and refractive index combination, a single layer of doped SiO_2 can already achieve the reflectivity minimum on these 3 semiconductor substrate at a given wavelength which can be calculated with the use of equation (6.1). We shall discuss all these applications in Chapter 6.

There can be various combinations of dopant concentration, substrate and processing conditions to suit various applications. Due to its stable native oxide, it is easier to design waveguide structures on Si than on GaAs or InP substrate. For the silicon technology, two main approaches have been used in the period from 1985 to date. In the first approach the high pressure thermal oxidation process is used to produce an isolation layer of about 5 μm, which is sufficient for infrared waveguide devices used for optical telecommunication [4.5]. In a second approach a flame hydrolysis deposition process is used to produce similar high quatity

layers [4.6]. Our work shows that the much simpler spin-on technology is capable of producing films of similar optical quality not only on Si, but also on GaAs and InP.

CHAPTER 5

FILM HOMOGENEITY AND MECHANICAL PROPERTIES

Solution deposited thin SiO_2 films with and without dopant can be used as antireflection coatings, waveguides and special overlays to protect the surface or control the refractive index and other properties of the underlying film or film substrate assemblies. For these applications, the thickness uniformity, homogeneity in the vertical direction and the mechanical properties of the films are critical. Often solution deposited films exhibit internal stress which is generally believed to be process related and depends on thermal expansion of the films and substrates used [5.2]. The removal of the organic solvent in the solution deposition process is also partly responsible for the stress. In this chapter we will first study the thickness uniformity and analyse the homogeneity in the vertical direction. The tensile stress is measured for pure and TiO_2 doped SiO_2 films. Also studied in this chapter are the etch rate characteristics of the films. Both plasma and chemical methods are used to etch the films as ways to control the film thickness.

5.1 FILM HOMOGENEITY

The film homogenieity in both the planar and in depth directions is considered in this paragraph. In our study we prepared two samples of SiO_2 and 1:1 SiO_2/TiO_2 on 2" silicon substrates following the method of Chapter 2 and then baked samples at 300°. Fig.5.1 is the thickness map of the 300°C baked SiO_2 film on a 2" diameter silicon wafer and Fig.5.2 is the corresponding map of the 1:1 SiO_2/TiO_2 film. Both pure and Ti-doped films show the same uniformity of flatness of about 1.2%.

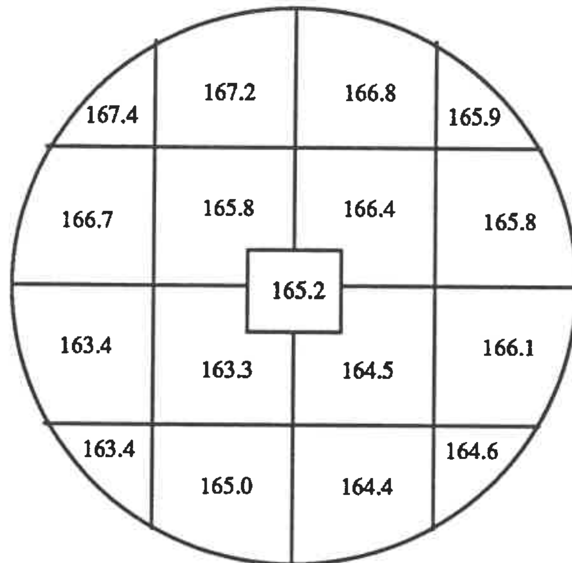

Fig.5.1 Thickness uniformity of a solution deposited silicon dioxide film on a 2" silicon wafer.

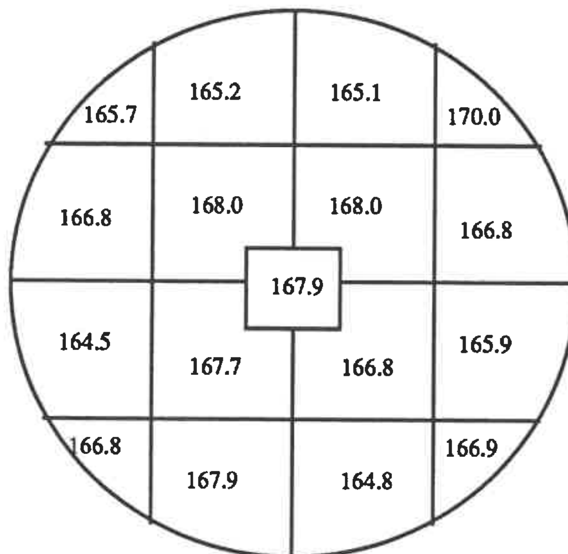

Fig.5.2 Thickness uniformity of a solution deposited SiO_2-TiO_2 film on a 2" silicon wafer.

As for the homogeneity in the vertical direction, compared to the surface uniformity, it is more difficult to measure. Our approach has been to associate variations in the normalised reflectance measurement at each point of the surface to variations in film thickness and optical constants. We look at the inhomogeneous film as a multilayer assembly on which we can use the mathematical approach developed in Chapter 3. Similar analyses for films on transparent substrates and for semiconductor films are carried out in reference [5.3] and [5.1]. In [5.3], the inhomogeneity influence on the reflectance of a film-glass assembly is studied. The work done in [5.1] is directed to the analysis of a semiconductor thin film on a heavily doped semiconductor substrate. The dopant diffusing out of the substrate during the film growth leads to inhomogeneity in the thin film and affects the reflectance of the resulting film substrate assembly. Both [5.1] and [5.3] assume a semi-infinitely thick and transparent or semitransparent substrate. In our simulation both transparent and absorbing substrates are treated and the general formulas developed in Chapter 3.2 are used to calculate the reflectance and normalised reflectance. The inhomogeneity in the vertical direction is assumed to be linear. In our analysis, the

vertically inhomogeneous is replaced by a set of staircased multilayers with the total sublayer thickness equal to the thickness of a single inhomogeneous film. When the number of sublayers is increased to eight or ten, the resulting reflectance of the staircased films approaches a constant value, and a further increase in the number of subdivisions have no influence on the values of the reflectance and normalised reflectance. So, in all our vertical uniformity simulations, the sublayer number is fixed at eight to obtain results of 1% accuracy. The refractive index configuration of the film substrate assembly we analysed is shown in Fig.5.3a. Fig.5.3b shows two normalised reflectance curves for two SiO_2 films with the same film thickness and the same degree of inhomogeneity but of different sign ($\Delta n/n_m$=+0.07,-0.07). The mean refactive index of the film, n_m, is assumed to be 1.40 and the film thickness is assumed to be 360 nm. The plus (or minus) sign in the inhomogeneity denotes that the film refractive index is linearly increased (or decreased) from the air-film interface to the film-substrate interface. From these simulated R_{norm}-λ curves, it can be seen that the effect of inhomogeneity is just to change the

R_{norm} maximum value, but not the position while the R_{norm} minimum point is constant. Thus the absolute value of the normalised reflectance maximum can be used as a measure of the film inhomogeneity and from the sign of the term $(1-R_{norm})$ we can determine whether the film's index of refraction is increasing or decreasing from the surface of the film towards the substrate interface. Since the general formula developed in Chapter 3 is used to analyse the inhomogeneity influence, these methods can also be used for other absorbing semiconductor or metal substrates.

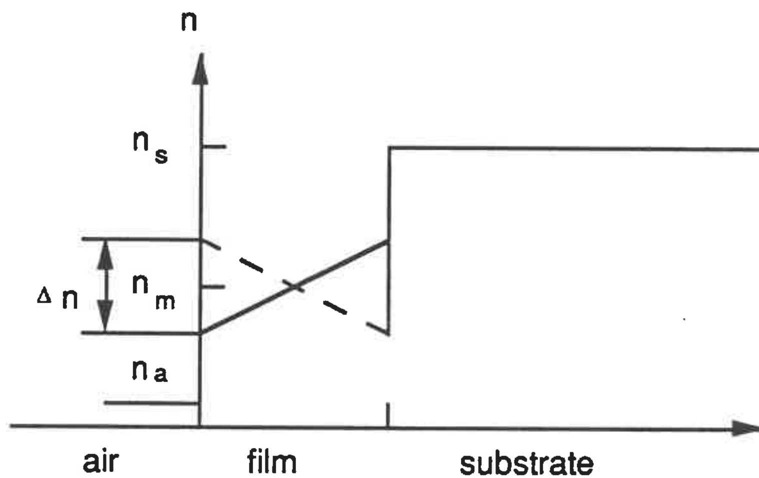

Fig.5.3a The air-film-substrate assembly and its refractive index.

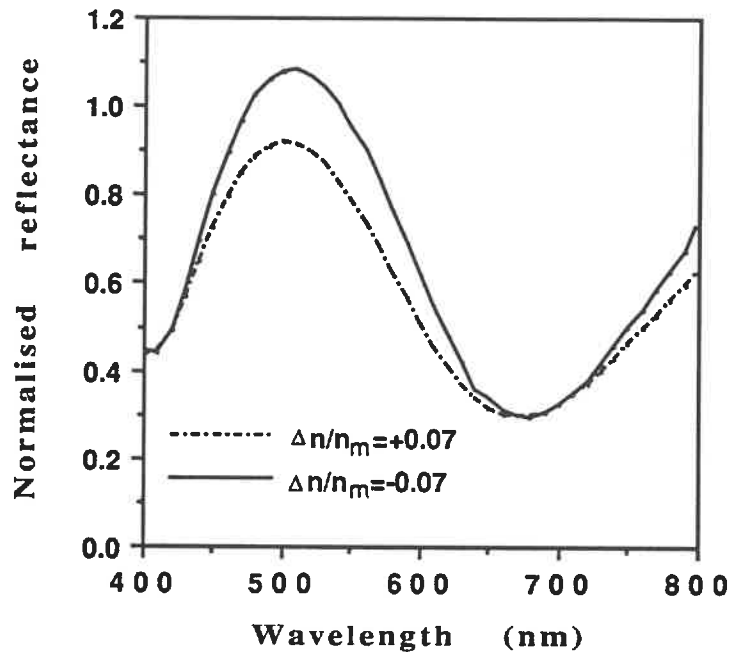

Fig.5.3b Calculated normalised reflectance as a function of wavelength for a film with thickness d=360 nm and n_m =1.4 for two different values of $\Delta n/n_m$ of 7% and -7% on silicon substrate.

Fig.5.4 plots calculated values of R_{norm} as a function of inhomogeneity as measured by $\Delta n/n$ for pure and TiO_2 doped silicon dioxide films on silicon. We note that there exists a linear relationship between the inhomgeneity and the normalised

reflectance changes and for pure SiO_2 films an inhomogeneity of 7% will cause the R_{norm} maximum change of about 10%. The R_{norm} of the well prepared solution deposited SiO_2 films rarely show deviations of R_{norm} maximum value great than 5% as the results in Chapter 4 demonstrate. From these simulations it can be concluded that the inhomogeneity in the vertical direction in our spin-on films is less than 5%. Our simulation for films on transparent substrates yields similar results as those of reference [5.3]. We have shown that the subdivision into eight layers is sufficient and the reflectance minimum is a measure of the inhomogeneity whereas the reflectance maximum is dependent just on the value of mean refractive index n_m and independent of the degree of inhomogeneity in the vertical direction. Both simulation for transparent and absorbing substrates shows that for transparent films, the reractive index derived from the measured normalised reflectance minimum is the mean refractive index when the film is inhomogenious in the vertical direction.

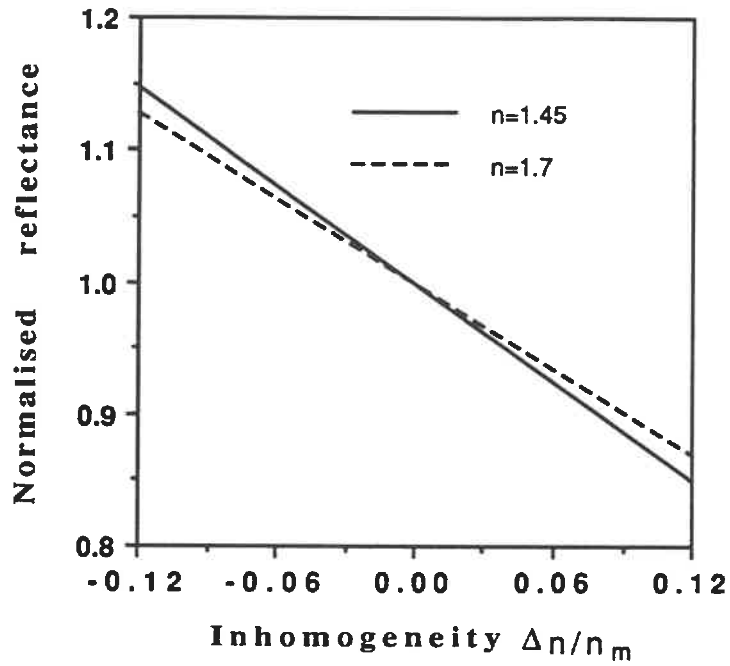

Fig.5.4 The film inhomogeneity in the vertical direction and the normalised reflectance relationship for solution deposited SiO_2 on silicon.

5.2 THE TENSILE STRESS

The stress introduced by the difference between the substrate expansion coefficient and that of the film after various steps of processing can be measured by the substrate-film composite bending [5.4]. If the substrate is assumed to be elastically homogeneous and the film thickness is much less than that of the substrate and under the influence of the film's bending moment the substrate assumes a spherical shape, then the length of substrate z, the radius of curvature ρ and the stress along the substrate length can be related [5.4]. Equating the substrate and the film's bending moments we can get a formula for the film's mean stress:

$$\sigma_f=(E/(1-\nu))\ (h^2/6t\rho) \qquad (5.1)$$

Thus from the measurement of ρ, we can deduce the mean tensile stress of the film. We use the Dektak surface profilometer to measure the surface bending of the SiO_2 films on silicon substrate. Contrary to the thermal oxide's compressive film stress, the

solution deposited method show a stress of opposite sign. Table 5.1 is the measurement results of solution deposited thin flms on 2" silicon wafers. Results show that the TiO_2 concentration influence upon the tensile stress is much greater than the temperature influence. This is in agreement with the observation that to obtain crack free films we must use low TiO_2 concentrations and the low temperature processing. The Ti rich films can be obtained using diluted solution and if the same processing is carried out we get much thinner films.

Table 5.1 the tensile stress of solution deposited SiO_2 and TiO_2/SiO_2 thin films on silicon (dynes/cm^2).

Films	Tensile stress	
	300 °C	500 °C
SiO_2	$2*10^9$	$6*10^9$
1:1 TiO_2/SiO_2	$13*10^9$	$17*10^9$

5.3. ETCH RATE OF THE FILMS

Beyond the optical properties of the spin-on films, it is important to establish the ease with which the films can be patterned after deposition and annealing steps. To this end the films have been etched using a CF_4 reactive etch process (CF_4: 25 mTorr, input power density: 0.548 W/cm2). The chemical etching method is also carried out to investigate the difference between the two methods. Fig.5.5 shows the plasma etch rates we obtained depend on the annealing temperature of the spin-on films. We note that the films are increasingly dense as we observed in terms of the index of refraction (see Fig.4.3).

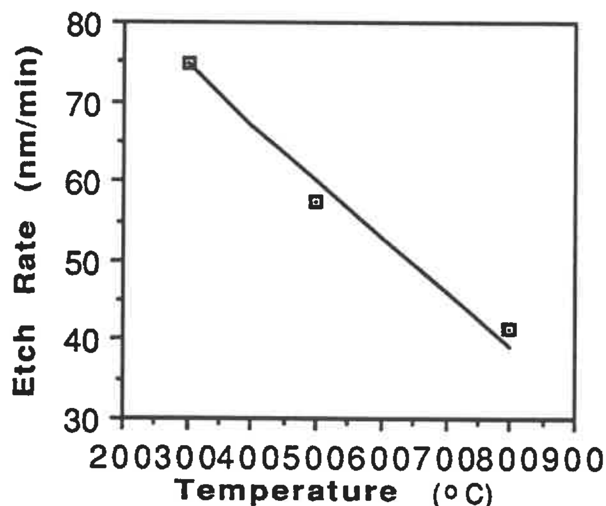

Fig.5.5 Plasma etch rate of silicon dioxide films baked at different temperature.

For the chemical method with conventional HF and NH_4F combination, the etch rate of low temperature baked solution deposited SiO_2 is much quicker than the thermal grown silicon dioxide, as some of the anode oxidation grown films show. To get a strict control, dilute etch solutions are used. Table 5.2 is the etch rate of solution deposited pure and Ti doped SiO_2 films fabricated on silicon substrate by a 1% 1:1 HF and NH_4OH solution. The high and uneven etch rate we found at 300 ^oC is probably due to a porous film sucture as has been previously observed microscopically [4.2].

Table 5.2 Etch rate of solution deposited thin films in HF/NH_4OH solution.

Composition	Baking temperature (℃)	Etch rate (nm/min)
SiO_2	300	> 1000
SiO_2	500	627.2
SiO_2	800	25.9
1:1 SiO_2/TiO_2	500	214.6
3:7 SiO_2/TiO_2	500	85.9
TiO_2	500	5.5
SiO_2 native oxide on silicon	1100	20.0

It is noted that the 800°C baked SiO_2 films show almost the same etch rate as the thermal grown native SiO_2 films. The Ti doping slows down the etch rate when the Ti content surpasses 50%. Finally, the Ti doping on the etch rates of spin-on films by plasma has been explored. Fixing the anneal temperature at 500°C, the etch rate of mixed TiO_2/SiO_2 spin-on films have been measured and are shown in Fig.5.6.

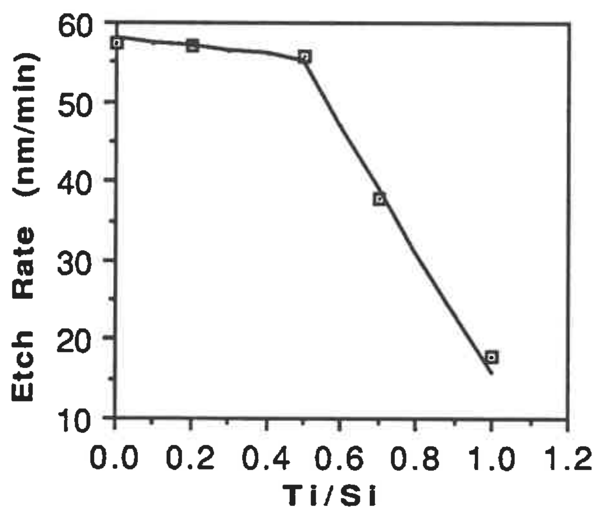

Fig.5.6 Plasma etch rate of silicon dioxide-titanium dioxide films.

We note that the TiO_2 concentration has little effect on the etch rate up to a 50% concentration, after which the etch rate drops

sharply, and proportionately with the TiO_2 concentration to a value of 18 nm/min.

Both the CF_4 plasma etch rate and the chemical etch rate experiment give us an indication that the 800 °C baked spin-on SiO_2 film becomes as dense as the thermally grown SiO_2. This is consistent with our refractive index measurement of these films and with the published result of the structural analysis of Ref. [5.5] for optical fibre preforms fabricated by a sol-gel process.

CHAPTER 6

ANTIREFLECTIVE, PROTECTIVE AND WAVEGUIDE APPLICATIONS

If properly processed and designed the SiO_2 thin films obtained by various methods should, to some degree, show the same properties and sometimes could replace one another. But actually all method has its own particularities, taking other factors such as economy into acount, we find that each method has its own merit and disadvantages for a special application. The solution deposited silicon dioxide films are formed at relatively low temperatures and can be doped easily with titanium dioxide to get films of different composition and refractive index. This is very useful for the optoelectronic application to make waguides. The low temperature processing also enables us to get an anti-reflection layer easily for semiconductor or glass substrate. In this chapter several examples are shown and discussed.

6.1 ANTIREFLECTION LAYER

For a transparent substrate such as glass (n=1.512), there always exist a reflectance of about 4% at visible or near infrared wavelengths. If we want to decrease this reflectance to zero or as low as possible at a wavelength, λ, of interest, a film with thickness of $\lambda/4$ and with refractive index given by (6.1) is necessary:

$$n_f = (n_a * n_s)^{1/2} \tag{6-1}$$

Unfortunately, there exists no such material with index of refraction of 1.23. But we can use two layers to get an admittance match and obtain zero reflectance at a selected wavelength of interest. For zero reflectance at normal incidence for two 1/4 λ layers acording the analysis at Chapter 3 we must have:

$$(n_{f2}^2 * n_s / n_{f1}^2) = n_a$$

If we use solution deposited SiO_2 as the second layer, the refractive index of the first layer must be 1.72 for perfect antireflection

match, as fig.6.1 shows. Solution deposited SiO_2 doped with titanium oxide shows a refractive index in the range from 1.4 to 2.0, it can well suit this kind of application.

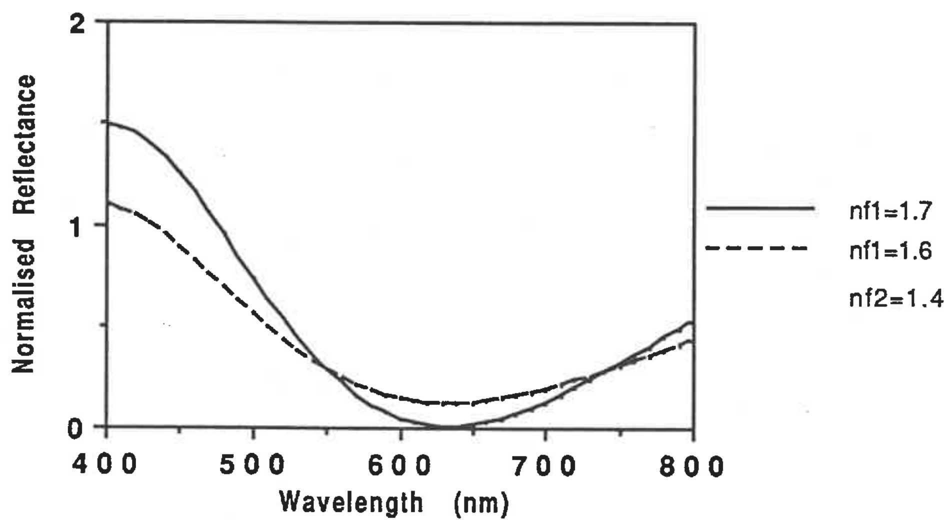

Fig.6.1 Two layer anti-reflection layer on glass.

As for most semiconductors, without an anti-reflection layer their reflection of about 30 % is too great for most applications. Single transparent layers can reduce this reflection considerably across the optical spectrum and particularly at specific wavelengths corresponding to interference. As an example, we have studied coatings of TiO_2 doped SiO_2 spin-on films for silicon. Fig.6.2

is an example. A 77.6 nm thick pure TiO_2 film on Si can effectively reduce the normalised reflectance to less than 0.05% at λ=633 nm, that of the emission wavelength of a He-Ne laser.

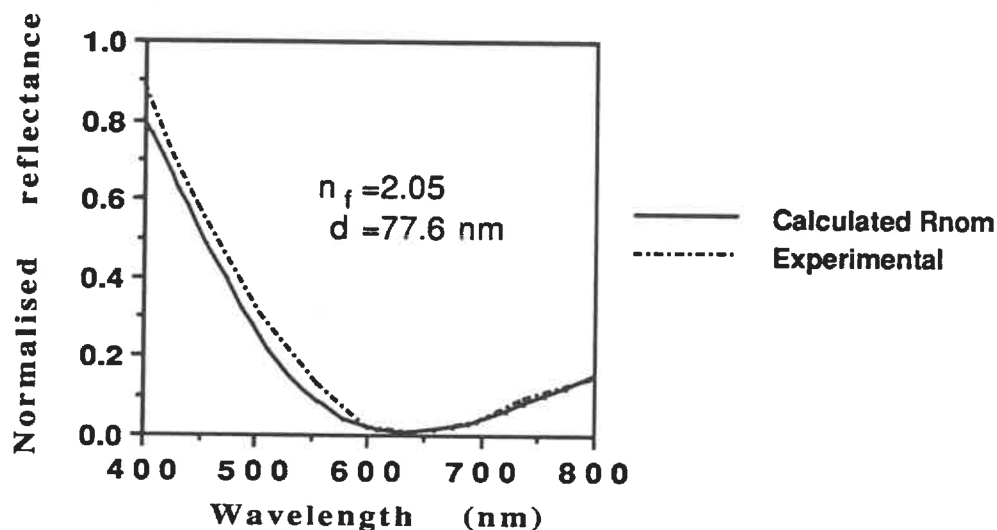

Fig.6.2 Single layer anti-reflection films on silicon.

For a broad band anti-reflection film on semiconductor substrates, a multi-layer structure is needed and the simulation can be carried out with the use of equations developed in Chapter 3.

6.2. PROTECTIVE LAYERS

The silicon dioxide layer can be used to protect a metal

surface against corrosion. In [6.4], it is found that solution deposited silicon dioxide shows a better protecting ability than plasma deposited silicon dioxide for silver thin films. Also, some thin metal films like gold are semi-transparent in the visible, and reflecting in the infra-red; so, for a silicon dioxide based multi-layer assembly with a very thin metal film, it is possible to get at the same time protection and enhanced transmittance at visible wavelengths. The addition of silicon dioxide films do not influence the normalised reflectance at infrared greatly. The solution deposited silicon dioxide can adhere to most metals such as aluminium, gold, copper and silver and can be used in combination with these metals to achieve some special effect such as a solar absorber [6.3]. There also exists several other applications for dielectric and thin metal film combinations in optics such as a beam splitter [6-3]. To show that silicon dioxide based films can well suit these applications, it is important that one can produce and measure accurately the thickness and refractive index on these metal films. Fig.6.3 is an example of a silicon dioxide thin film deposited on an evaporated aluminium film.

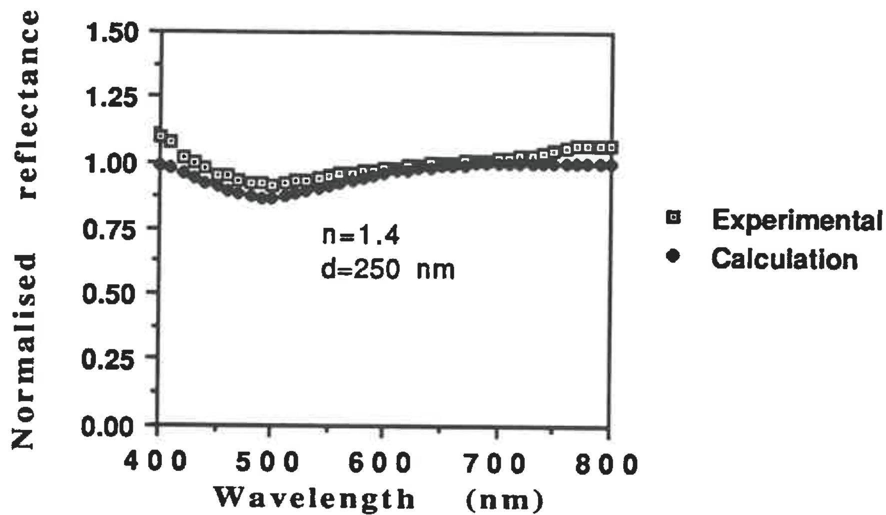

Fig.6.3 Normalised reflectance of SiO_2 film on aluminium.

Note that the introduction of a SiO_2 layer on top of an aluminium film does not change the reflectance of the film greatly.

6.3.1 WAVEGUIDES

The solution deposited silicon dioxide doped with titanium dioxide has a refractive index in the range of 1.4-2.0 and is suited for the fabrication of waveguides. Planar waveguides on glass are tested. The light is coupled through a prism into the planar

waveguide and the effective refractive index of the resulting planar waveguide can be measured.

Several TiO_2 doped SiO_2 films on glass are produced and refractive index and the thickness of these waveguiding films are measured by the normalised reflectance method proposed in Chapter 3. The effective refractive index of the resulting planar waveguide n_e can be calculated from the measured d and n values of the films. The He-Ne laser prism coupling method [6.5] can also be used to get the n_e value. Results from these two methods are listed in Table 6.1 for several TiO_2/SiO_2-glass samples. Also from this table we conclde that TiO_2 doping is an effective way to control the films refractive index over a wide range. Combined with the thickness control of the spin-on method we can fabricate high performance waveguides with different effective refractive index values.

Table 6.1

Comparision of n_e data measured by the prism coupling method with results from our d-n calculation.

Films	Thickness:d Refractive index:n	n_e From n,d calculation	n_e Prism method
1:1 TiO_2/ SiO_2 300 ℃	d=310 nm n=1.70	1.59304	1.5944
1:1 TiO_2/ SiO_2 300 ℃	d=153 nm n=1.70	1.51835	1.51876
1:1 TiO_2/ SiO_2 150 ℃	d=280 nm n=1.62	1.52680	1.52643

From the table we conclude that the waveguide effective index measurement can also be used to accurately determine the refractive index, especially for films so thin as to have no maximum or minimum in the normalised reflectance spectrum.

We have performed the difficult thickness measurement on such a film-glass assembly and our results are shown on Fig.6.4.

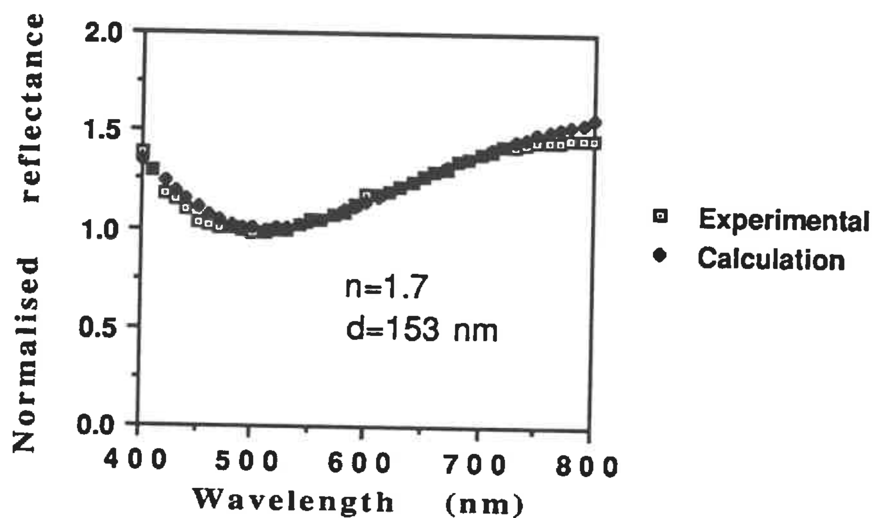

Fig.6.4 Normalised reflectance spectrum of SiO_2/TiO_2-glass assembly with SiO_2/TiO_2 layer thickness of 153 nm.

It is easy to show that for a transparent substrate of unkown optical constant, if we apply a film of known optical constant, one can derive the refractive index of the substrate from the minimum or maximum in spectrum of normalised reflectance of the film substrate assembly. When the substrate refractive index is greater

than that of film's we get minima less than 1, and when the substrate refractive index is smaller than that of the films we get maxima greater than 1. Fig.3.6 of Chapter 3 can be used to evaluate the substrate refractive index. For the absorbing substrate either the k or the n of the substrate must be known to determine the other. Otherwise a seperate transmittance experiment must be done on the same substrate as in the case of metal films discussed at [6.4].

6.3.2 COUMARIN DOPED SOLUTION DEPOSITED SiO_2

For integrated optics applications, it is useful to incorporate a colour center into a thin film such as SiO_2. We have used Coumarin 504 as a color center in the spin-on SiO_2 film and have studied the absorption and the fluorescence spectra. The Coumarin doped thin films are made by directly dissolving the Coumarin into the SiO_2 Liquicoat solution and then by applying this solution on potassium ion exchanged glass waveguides. Processing is completed as for the ordinary spin-on SiO_2 coatings. The Coumarin doped thin films are transparent and show a characteristic yellowish color. The color begins to fade at 200 to 300 ^{o}C of baking. The films always remain

transparent. Fig.6.5 is the waveguide absorption spectrum of a Coumarin doped SiO_2 film covered 10 micrometer potassium ion exchanged glass waveguide [6.5]. The film is baked at 150oC. The Coumarin concentration in the Liguicoat solution is 0.02 mole and the film thickness is 180 nm. In the wavelength range of 370-490 nm it shows absorption. The measurment is carried out using a system shown on Fig.6.6.

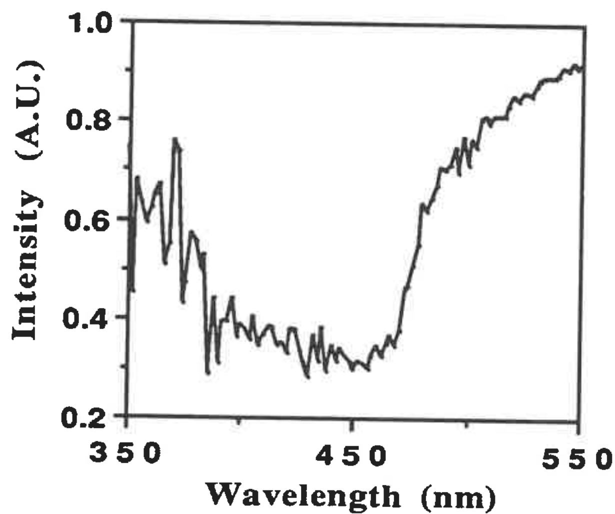

Fig.6.5 Absorption spectrum of a waveguide with Coumarin doped SiO_2 overlay.

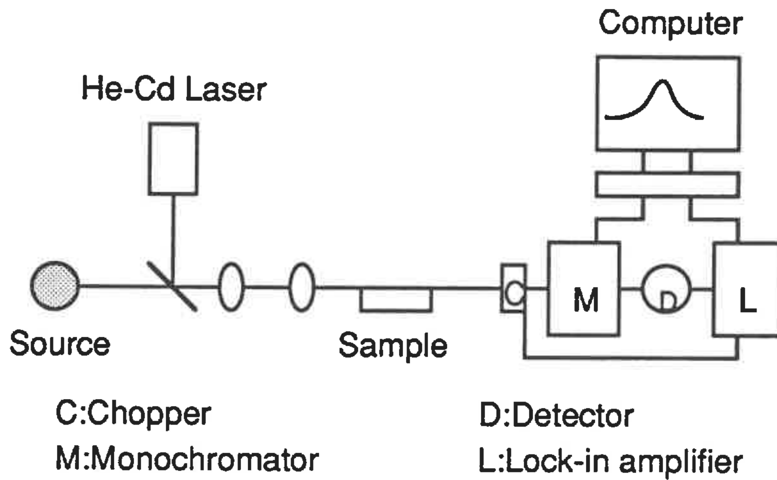

Fig. 6.6 System used for the measurement of waveguide spectrum characteristics.

We use a He-Cd laser of 5 mW output and a 40 X objective to couple the laser beam into the waveguide with a Coumarin doped solution deposited SiO_2 overlay. The excited photoluminescence is shown in Fig.6.7. The 40 nm breadth of the fluorescent spectrum make this film ideal for use as an active media in optical devices.

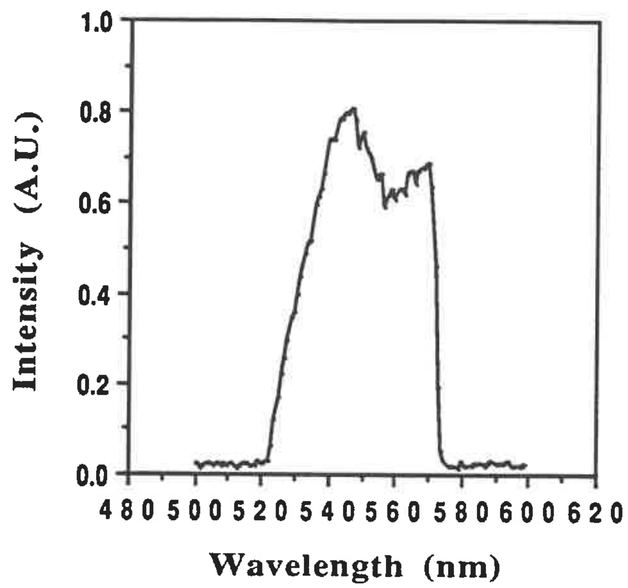

Fig.6.7 Fluorescence spectrum of a waveguide with Coumarin doped SiO_2 overlay.

6.3.3. In_2O_3/P_2O_5 DOPANT

P_2O_5 is widely used as a dopant to compensate the mobile ion effect in SiO_2 systems. In [6.6] the P_2O_5 doped solution deposited SiO_2 is used as an intermediate layer on top of $LiNbO_3$ substrate. The introduction of P_2O_5 decreases drastically the drift current in the layer and makes the whole device more stable.

In this work we have studied a P_2O_5-In_2O_3 dopant which can be a transparent material in the film form by itself. The film is prepared as introduced in Chapter 2 . The index of refraction and the thickness of the film is measured on the semiconductor surface using the reflectance minimum method developed in Sec. 3.1. Since its index of refraction is greater than that of glass substrate, the reflectance maximum is used to analyse the normalised reflectance data and to to get the thickness and the index of refraction of the film on glass substrate.

It is noted that for a material with P_2O_5/In_2O_3=1.25/1, the processing temperature is low. Fig.6.8 is the processing temperature and thickness relationship for a film spin-on coated on a silicon

surface. The low temperature processing corresponds to a temperature of 200° C at region b on Fig.2.1.

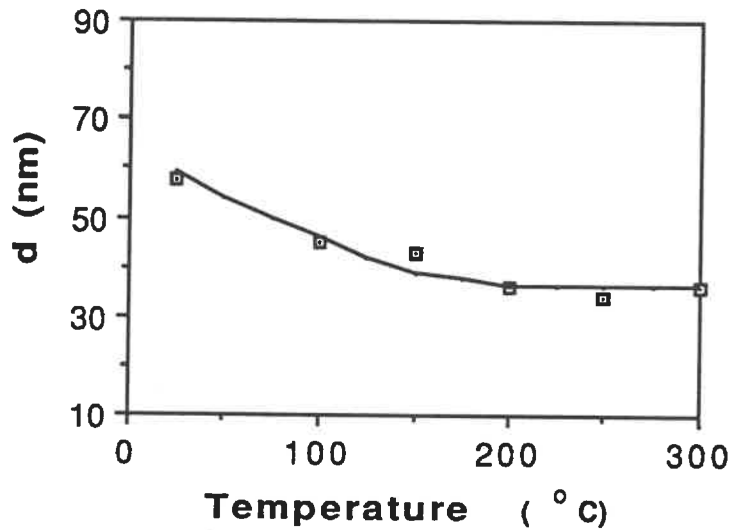

Fig.6.8 The processing temperature and film thickness relations of a 1.25:1 P_2O_5/In_2O_3 thin films.

Fig6.9 shows the dispersion curve we obtained by the normalised reflectance minimum method.

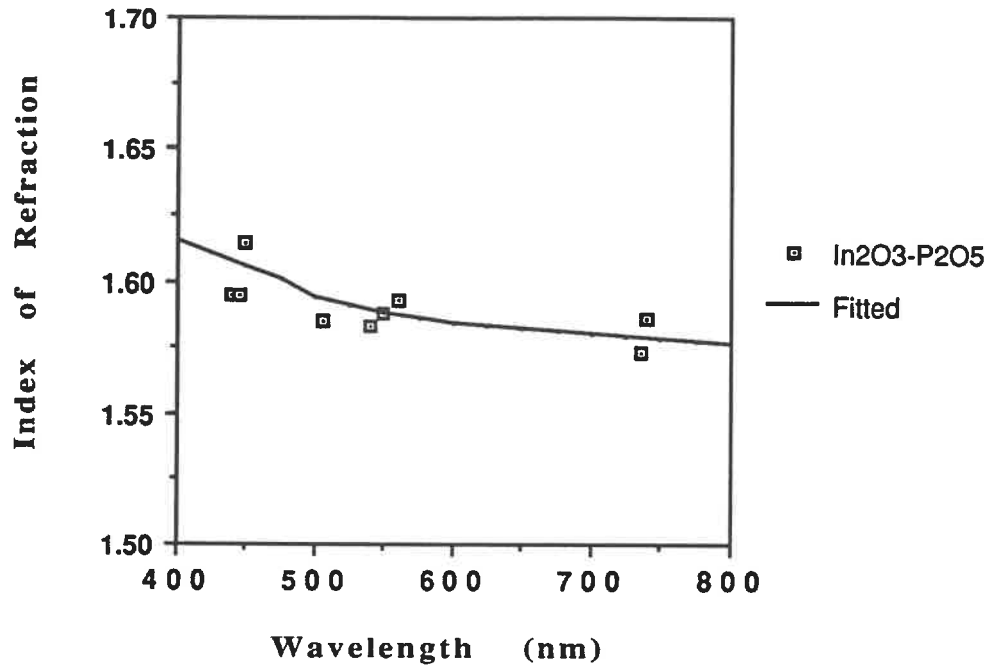

Fig.6.9 Dispersion curve of solution deposited 1.25:1 P_2O_5/In_2O_3 thin films.

The solution can readily adhere on glass and InP surfaces, less readily on silicon surfaces. Fig.6.10 is a normalised reflectance spectrum of a 1.25:1 P_2O_5/In_2O_3 films on Si. Also shown in this Fig. are simulated curves using data from Fig 6.9.

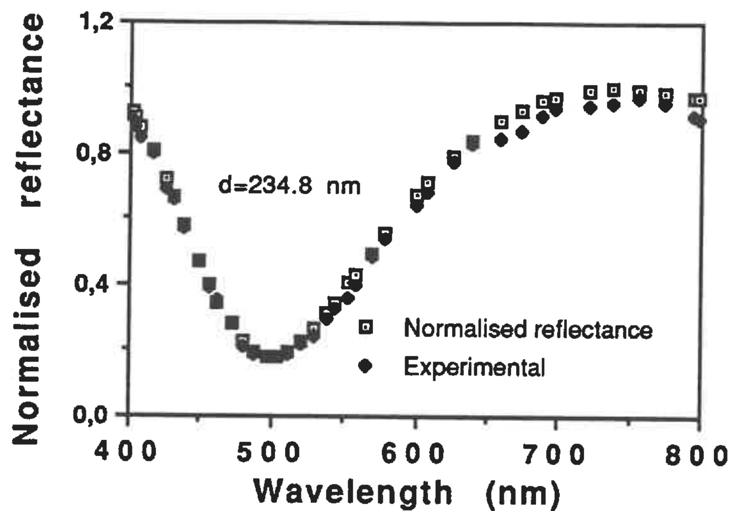

Fig.6.10 Normalised reflectance spectrum of a 234.8 nm thick 1.25:1 P_2O_5/In_2O_3 film on Si substrate.

Preliminary experiments show that the films on glass show waveguiding properties. With its low temperature processing and its transparency in the visible wavelength range, this material can perhaps serve as a useful dielectric, especially on InP substrates. The potential uses of this material are diffusion masks and passivation layers.

CHAPTER 7

CONCLUSION

In this thesis we have studied the characteristics of pure and doped solution deposited thin SiO_2 films and their applications. We have used the spin-on method to produce pure and doped SiO_2 films for integrated optics and microelectronics.

The relationship of processing parameters and the characteristics of the film obtained has been studied. Among the characteristics we studied are film refractive index and the film thickness homogeneity.

Using the characteristic matrix notation [3.6], a normalised reflectance method is developed and used to determine at the same time film thickness and refractive index both on glass and semiconductor surfaces. For this sake, a general normalised reflectance calculation is carried out to suit various film substrate combinations, including both transparent films, absorbing films and multilayers. The practical software is written in MATHCAD notation and is especially well suited to the various thin film calculations.

For single transparent layers on semiconductors, a minimum in the normalised reflectance spectrum can at the same time give the film thickness and the refractive index at a particular wavelength, using equation (3.8b) and Fig.3-2. We have in course of this thesis work developed a technique based on the measurement of the normalised reflectance and its mathematical and numerical treatment. Our method is more accurate than many widely used at this time such as the method of Ref. [3.4], which neglects k of the substrate and uses equation (3.9b). Using numerical calculation at wavelengths shorter than 500 nm and/or when the film refractive index is greater than 1.50, we can reproduce measured spectra with a maximum error of 1% in normalised reflectance and deduce to within 0.01 the refractive index value. One uniqueness of our numerical algorithms and its software implementation with MATHCAD is for single layers, it can quickly and accurately give the normalised reflectance of the film-substrate assembly. A second minor, but useful originality is that for multi-layer calculations the layer sequence we used is that in accord of the physical processing sequence. The algorithm can readily be adapted to the semiconductor epilayer thickness analysis as measured by infrared reflectance or normalised reflectance. As

a test of the normalised reflectance measuement technique and analysis method, the refractive index of thermally grown SiO_2 on silicon was mesured and the results are in good agreement with reported data of [4.1]. The deviation between the calculated normalised reflectance value and the measured value is within 2.5%.

Using the spin-on technique we fabricated thin films of excellent quality. For example, the homogeneity in the x and y directions of 1.2% was achieved for both pure and 1:1 TiO_2 doped SiO_2 on silicon. The homogeneity in the vertical,or Z-direction was analysed with a multilayer model of 8 layers. Our work extended the work of [5.3] to absorbing substrates. It is found that the homogeneity in the Z-direction is 5%. We also find that for linearly inhomogeneous films, the refractive index we derived from the reflectance minimum method is the mean refractive index as calculated by averaging through the depth of the inhomogeneous film.

The etch rates of the films are measured using both plasma and chemical methods. These experiments are in agreement with our refractive index measurements. The 800 ^{o}C baked SiO_2 has essentially the same etch rate as that of thermally grown SiO_2 on silicon.

The films stress on silicon wafers was measured by the composite bending method. We found that for the film stress on silicon, the TiO_2 concentration influence is greater than the temperature influence. Thus, to obtain TiO_2-rich films, diluted solutions need be used.

The spin-on films were tested as antireflection coatings on semiconductor surfaces. We found that at a specified wavelength of interest, a single layer of TiO_2 rich film is sufficient to obtain an essentially reflectionless surface.

The TiO_2 doped SiO_2 films were used to make waveguides. We measured the effective refractive index of the waveguide and compared it with the value we had determined by normalised reflection and n-d calculation. The two methods agree perfectly to within experimental error. The TiO_2 concentration and film thickness control enables us to obtain waveguiding films with various effective refractive index values.

We have successfully used Coumarin 504 to dope spin-on SiO_2, and used these films to overlay ion-exchanged glass waveguides. We measured the absorption spectrum and the fluorescence at the output of the glass waveguide. We successfully demonstrated that an

organic dye can be incorporated into an inorganic matrix and show broad fluorescence spectrum, creating an optical medium with gain.

BIBLIOGRAPHY

1

[1.1] R. J. Speer, "Organic compounds of titanium. I. Tetraalkyl orthotitanates", J. Organic Chemistry, 14, 655-659, (1949).

[1.2] E.S.Schlegel, "A bibliography of metal-insulator-semiconductor studies", IEEE Trans. Electron Devices, ED-14 (11), 728-49 (1967).

[1.3] E.Kooi,Surface properties of oxidized silicon, Springer- Verlag, New York, (1967).

[1.4] E.S.Schlegel, "Additional bibliography of metal-insulator-semi-conductor studies", IEEE Trans. Electron Devices, ED-15 (12),851-4 (1968).

[1.5] H.Schroeder,in "Physics of thin films",vol.5, Ed. by G.Hass, R.E.Thun, Academic Press Inc., New York, p87,(1969).

[1.6] H. A. Macleod, "Thin film optical filters", Adam Hilger Ltd, London, 3, (1969).

[1.7] R.Bruckner, "Properties and structure of vitreous silica". J. Non-Crystalline Solids, 5, 123-75 (1970).

[1.8] L.I.Maissel and R.Glang, (Eds.), Handbook of thin film

technology, McGraw-Hill Book Company, New York, 1970.

[1.9] J.W.Diggle, (Ed.), Oxides and oxide films, Volume 1, Marcel Dekker, Inc., New York, (1972).

[1.10] M.J. Rand, D.R.Standley,"Silicon oxynitride films on fused silica for optical waveguides", Appl. Opt., 11, 2482-2488, (1972).

[1.11] R. Ulrich, H.P. Weber,"Solution deposited thin films as passive and active light guides", Appl. Opt., 11, 428-434, (1972).

[1.12] J.W. Diggle, (Ed.), Oxides and oxide films, Volume 2, Marcel Dekker, Inc., New York, (1973).

[1.13] D. L. Pulfrey, J. J. H. Reche, "Preparation and properties of plasma-anodized silicon dioxide films", Solid Electronics, 17,627-632 (1974).

[1.14] W. Stutius, W. Streifer, Appl. Opt.,16,3218,(1977).

[1.15] A. H. Agajanian, "A bibliography on silicon dioxide films", Solid State Technology, Jan, 36-46 (1977).

[1.16] R.W. Philips and J.W. Dodds, Appl. Opt. 20, 40,(1981).

[1.17] K. Tiefenthaler, W. Lukosz, "Integrated optical switches and

gas sensors", Optics Letters,10,137-139, (1984).

[1.18] D.W. Hewak, J.W.Y. Lit,"Standardization and control of a dip-coating procedure for optical thin films prepared from solution", Can. J. Phys .66, 861-867,(1988).

2

[2.1] H. Schroeder, in "Physics of Thin Films", Vol.5, Ed. by G. Hass, R.E.Thun, Academic Press Inc., New York,(1969).

[2.2] R. Ulrich, H.P. Weber, "Solution deposited thin films as passive and active light guides", Appl. Opt.,11, 428,(1972).

[2.3] P.Herrman, D.Wildmann, "Fabrication of planar dielectric waveguides with high optical damage threshold", IEEE J. of Quantum Electronics, Vol. QE-19, 1735-1738, (1983).

[2.4] J.A. Moreland, "The Technology of Crystal and Slice Shaping", in "VLSI Electronics Microstructure Science", vol.12 Ed. N.W. Einsprunch and H. Huff, Academic Press Inc. p.83, (1985).

[2.5] E.Merk, Liquicoat Si ZLI 2123 and Liquicoat Ti ZLI 1857, product data sheet.

[2.6] P.Shen, M.J. Li, S.I. Najafi, J.F. Currie and R.Leonelli, " Optical and mechanical characterization of spin-on deposited silicon and

titanium oxide films", SPIE's1990 International Symposium on Optical and Opto-Electronic Applied Science and Engineering, vol.1328, paper 33, San Diego, July, (1990).

3

[3.1] O.S. Heavens, "Optical properties of thin solid films", Academic Press Inc., p.160,(1955).

[3.2] J.A. Berning and P.H. Berning, J. Opt. Soc. Amer. 50, p.813 (1960).

[3.3] M. Born and E. Wolf, "Principles of Optics", 3rd., P.632, Pergamon Press Inc., New York,(1965).

[3.4] I. Franz and W. Langheinrich, "A simple non-destructive method of measuring the thickness of transparent thin films between 10 and 600 nm", Solid State Electronics, 11, 59-64, (1968).

[3.5] L.J. Fried and H.A. Froot, "Thickness measurement of silicon dioxide films over small geometries," J. Appl. Phys. 39, 5732-5735, (1968).

[3.6] H.A. Macleod, "Thin film optical filters", Adam Hilger Ltd., London, (1969).

[3.7] G. Hass, M.H. Farancombe and R.W. Hoffman, ed., "Physics of thin

films", Vol.9,73-144. (1977).

[3.8] J.P. Borgogno, B. Lazarides and E. Pelletier, "Automatic determination of the optical constants of inhomogeneous thin films", Applied Optics, 21, 4020-4029, (1982).

[3.9] S.B. Kulkarni, "Characterization of silicon epitaxial films", in " VLSI Electronics Microstructure Science", N.G. Einspruch, Ed. Academic Press, Vol.6, p.112, (1983).

[3.10] J. Gowar, "Optical Communication Systems", Prentice/Hall International, p.44, (1984).

4

[4.1] I.H. Maltson,"Inter-specimen comparison of refractive index of fused silica", J. Optical Soc. of America 55, 1205-1209,(1965).

[4.2] R.W. Philips, J.W. Dodds, "Optical interference coatings prepared from solution", Appl. Opt. 20, 40-47, (1981).

[4.3] J.Gowar, "Optical Communication Systems", Prentice/Hall International, 44, (1984).

[4.4] E.D. Palik, Ed. "Handbook of Optical Constant of Solids", Academic Press Inc., D.F.Edwards, "Silicon", p.547. E.D.Palik, "Gallium arsenide" , p.429. D.J.Glembocki, H.Piller, "Indium

phosphide", p.503, (1985).

[4.5] C.H. Henry, R.F. Kazarinov, H.J. Lee, K.J. Orlowsky, and L.E. Katz, "Low loss Si_3N_4-SiO_2 optical waveguides on Si", Applied Optics, 26, 2621-2624, (1987).

[4.6] D.W. Hewak, J.W.Y. Lit, "Fabrication of tapers and lenslike waveguides by a microcontroled dip coating", Applied Optics, 27, 4562-4564, (1988).

[4.7] Y. Hbino, T. Kitagawa, M. Shimizu, F. Hanawa, and A. Sugita, "Neodymium-doped silica optical waveguide laser on silicon substrate", IEEE Photonics Technology Letters, vol.1, 349-350, (1989).

5

[5.1] T. Abe and T. Kato, "Infra-red reflectivity of N on N+ Si wafers", Jpn. J. Appl. Phys. 4, 742 (1965).

[5.2] R.S.Sokolova, "Internal Stresses in thin oxide films deposited from hydrolyzable solutions", Optical Technology, 41, 1, 15-17, (1974).

[5.3] J.P. Borgogno, B. Lazarides and E. Pelletier, "Automatic determination of the optical constants of inhomogeneous

thin films", Applied Optics, 21, 4020-4029, (1982).

[5.4] A.Segmuller and M.Murakami, "X-ray diffraction analysis of strains and stresses in thin films", in "Analytical Techniques for Thin Films", K.N. Tu and R. Rosenberg, Ed., 162-163, Academic Press,Inc., (1988).

[5.5] A.M. Elias, M.E. Elias, M.M. Nunes, "Structural analysis of optical fibre preforms fabricated by sol-gel process", in " Acoustic, Thermal Wave and Optical Characterization of Materials", European Materials Research Society Symposia Proceedings, Vol. 11, 393-397, (1990).

6

[6.1] T. Abe and T. Kato, "Infra-red reflectivity of N on N+ Si wafers", Jpn. J. Appl. Phys. 4, 742 (1965).

[6.2] P.K. Tien, R. Ulrich, R.J. Martin, Appl. Phys. Lett. 14, 291 (1969).

[6.3] J.C.C. Fan, F.J. Bachner, G.H. Foley, P.M. Zavracky, "Transparent heat mirror films of $TiO_2/Ag/TiO_2$ for solar energy collection and radiation insulation", Appl. Phys. Lett., 25, 12, 693 (1974). J.C.C. Fan, F.J. Bachner, "Transparent heat mirrors for solar energy applications", Appl. Opt. 15, 4, 1013 (1976).

[6.4] R.W. Philips, J.W. Dodds, Applied Optics, 20,40, (1981).

[6.5] Iraj S. Najafi, Min-jung. Li, "Ion-exchanged glass integrated optical components", Invited Paper, IEEE International Workshop on Photonics, Networks, Components and Applications, Montebello, October, (1990).

[6.6] T. Suhara, M. Fujimura, K. Kinoshita, H. Nishihara," Reduction of DC drift in $LiNbO_3$ waveguide electro-optic devices by phosphorus doping in SiO_2 buffer layer", Electronics Letters, 26, 17, 1409-1410, (1990).

[6.7] A.M. Elias, M.E. Elias, M.M. Nunes, "Structural analysis of optical fibre preforms fabricated by sol-gel process", in " Acoustic, Thermal Wave and Optical Characterization of Materials", European Materials Research Society Symposia Proceedings, Vol. 11, 393-397, (1990).

APPENDIX

APPENDIX 1

OPTICAL CONSTANTS OF Si, GaAs AND InP

The optical constant of Si, GaAs and InP are taken from reference [4.4] and compiled in the matrix form in the MATHCAD notation. Combined with Appendix 2, it become a programm which can simulate the normalised reflectance minimum of transparent thin film and semiconductor combination.

Appendix.1.1- Silicon Optical Constant

$i := 0 ..37$

$\lambda :=$	$ns :=$	$ks :=$
400	5.570	0.387
403	5.493	0.355
407	5.349	0.313
416	5.164	0.255
425	5.009	0.211
431	4.916	0.194
439	4.791	0.170
449	4.682	0.149
456	4.615	0.131
462	4.553	0.131
473	4.466	0.120
480	4.416	0.094
488	4.367	0.079
496	4.320	0.073
504	4.277	0.066
512	4.235	0.060
521	4.196	0.056
530	4.159	0.043
539	4.123	0.048
544	4.106	0.044
554	4.073	0.032
559	4.042	0.032
569	3.997	0.027
579	3.969	0.030
596	3.943	0.025
608	3.918	0.024
626	3.893	0.022
639	3.870	0.018
660	3.847	0.016
674	3.815	0.014
689	3.796	0.013
697	3.778	0.012
721	3.761	0.011
738	3.745	0.010
756	3.728	0.009
775	3.721	0.008
795	3.705	0.007
800	3.688	0.006

Appedix.1.2- GaAs Optical Constant

$i := 0 \,..37$

$\lambda :=$	ns :=	ks :=
400	4.373	2.146
405	4.439	2.029
411	4.483	1.961
416	4.550	1.952
425	4.755	1.960
427	5.052	1.721
434	5.102	1.353
440	5.015	1.085
446	4.902	0.912
453	4.793	0.789
456	4.741	0.739
462	4.649	0.659
470	4.567	0.595
477	4.492	0.539
484	4.423	0.497
492	4.362	0.458
500	4.305	0.426
508	4.254	0.398
517	4.205	0.371
530	4.141	0.337
544	4.082	0.308
559	4.029	0.285
569	3.998	0.266
579	3.968	0.251
596	3.927	0.232
608	3.904	0.223
626	3.867	0.203
639	3.846	0.187
660	3.817	0.173
674	3.799	0.168
689	3.785	0.151
697	3.779	0.152
721	3.752	0.118
738	3.734	0.105
756	3.716	0.097
775	3.700	0.091
795	3.685	0.087
800	3.679	0.085

Appendix.1.3-InP Optical Constant

$$\lambda := \begin{bmatrix} 400 \\ 408 \\ 413 \\ 421 \\ 427 \\ 437 \\ 443 \\ 452 \\ 459 \\ 470 \\ 477 \\ 488 \\ 496 \\ 508 \\ 517 \\ 530 \\ 539 \\ 553 \\ 564 \\ 579 \\ 590 \\ 608 \\ 620 \\ 639 \\ 653 \\ 674 \\ 689 \\ 713 \\ 730 \\ 760 \\ 800 \end{bmatrix} \quad ns := \begin{bmatrix} 4.415 \\ 4.433 \\ 4.395 \\ 4.314 \\ 4.265 \\ 4.175 \\ 4.121 \\ 4.048 \\ 4.004 \\ 3.940 \\ 3.903 \\ 3.851 \\ 3.818 \\ 3.773 \\ 3.745 \\ 3.706 \\ 3.682 \\ 3.649 \\ 3.629 \\ 3.602 \\ 3.585 \\ 3.563 \\ 3.549 \\ 3.530 \\ 3.517 \\ 3.501 \\ 3.492 \\ 3.481 \\ 3.476 \\ 3.489 \\ 3.459 \end{bmatrix} \quad ks := \begin{bmatrix} 1.735 \\ 1.414 \\ 1.247 \\ 1.061 \\ 0.964 \\ 0.847 \\ 0.786 \\ 0.712 \\ 0.667 \\ 0.614 \\ 0.579 \\ 0.536 \\ 0.551 \\ 0.479 \\ 0.457 \\ 0.431 \\ 0.416 \\ 0.393 \\ 0.380 \\ 0.358 \\ 0.347 \\ 0.329 \\ 0.317 \\ 0.299 \\ 0.293 \\ 0.278 \\ 0.270 \\ 0.255 \\ 0.242 \\ 0.225 \\ 0.209 \end{bmatrix}$$

APPENDIX 2

THE NORMALISED REFLECTANCE MINIMUM OF THIN FILMS OF DIFFERENT REFRACTIVE INDEX ON Si, GaAs AND InP

The normalised reflectance minimum of transparent thin films of different refractive index and semiconductor combination are calculated using formular (3.1) to (3.8) . The optical constant are shown in Appendix 1. The results of the calculation of this Appendix can be used to find the refractive index of the transparent thin films from its normalised reflectance minimum values in a film-substrate's normalised reflectance spectrum.

$$\lambda(i) := \lambda_i \qquad ns(i) := ns_i \qquad ks(i) := ks_i$$

$$na := 1 \qquad j := 0 \,..\, 9 \qquad nf(j) := 1.40 + 0.05 \cdot j$$

$$r12(j) := \frac{nf(j) - na}{na + nf(j)} \tag{3.2}$$

$$p23(i,j) := \frac{\left[(ns(i) - nf(j))^2 + ks(i)^2\right]^{0.5}}{\left[(nf(j) + ns(i))^2 + ks(i)^2\right]^{0.5}} \tag{3.3}$$

$$R0(i) := \frac{(ns(i) - na)^2 + ks(i)^2}{(ns(i) + na)^2 + ks(i)^2} \tag{3.6}$$

$$Rm(i,j) := \frac{(p23(i,j) - r12(j))^2}{(1 - p23(i,j) \cdot r12(j))^2} \tag{3.8b}$$

$$R(i,j) := \frac{Rm(i,j)}{R0(i)} \tag{3.7}$$

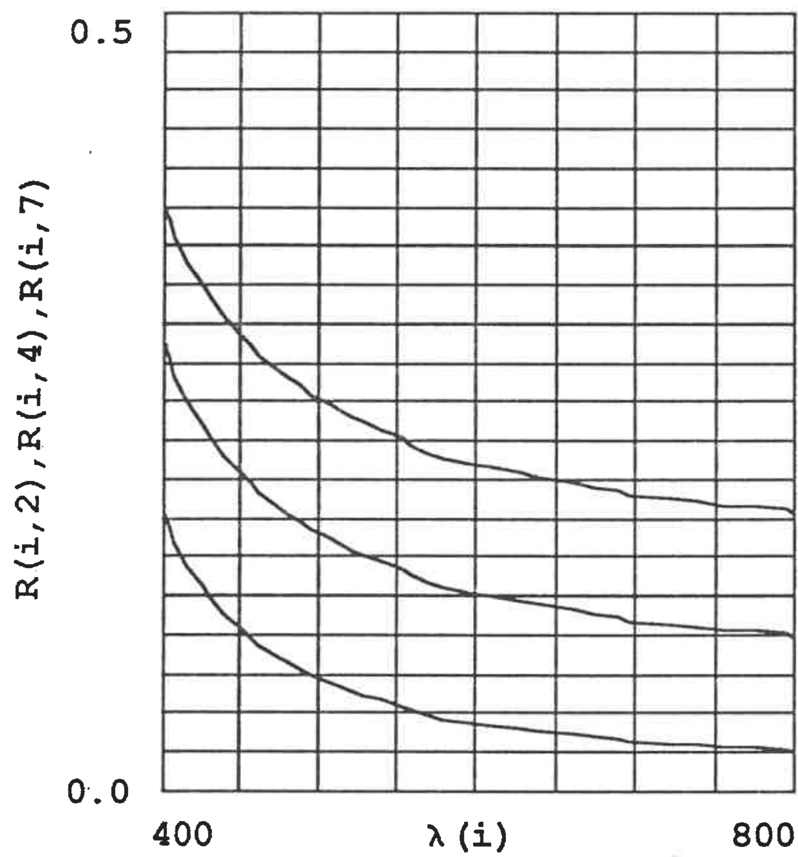
0.5
R(i,2),R(i,4),R(i,7)
0.0
400
λ(i)
800

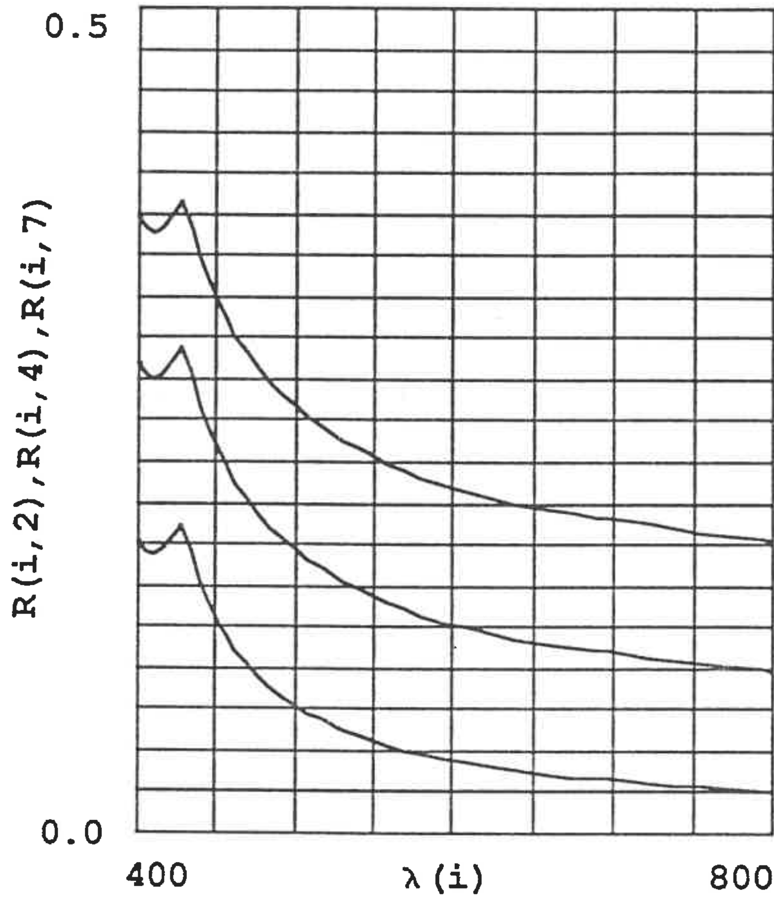

(nm)

GaAs

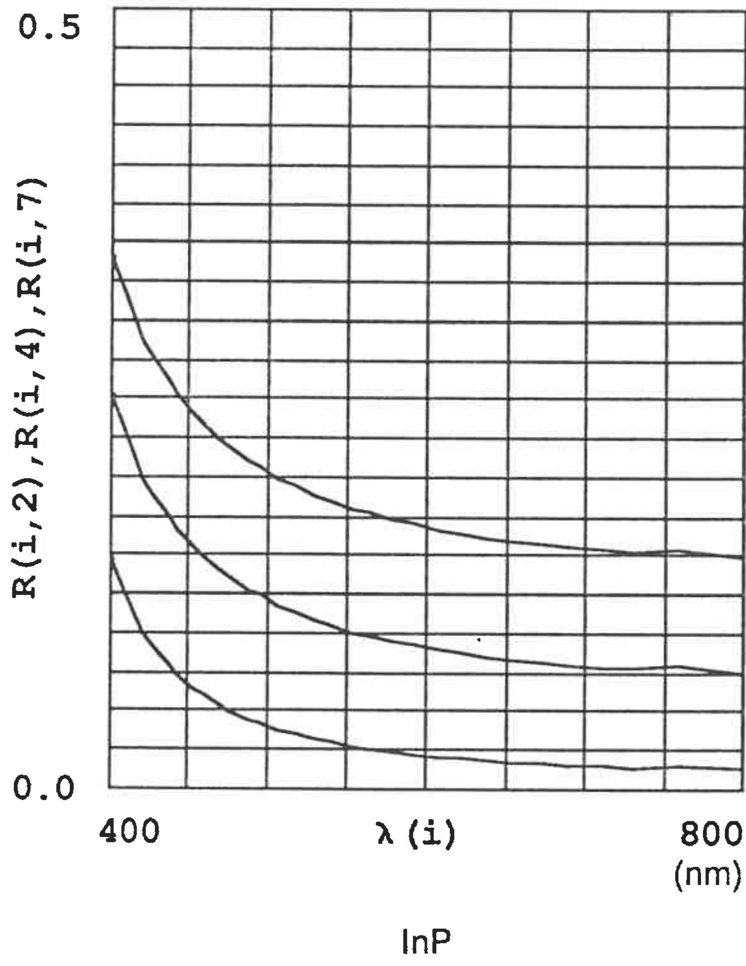

InP

APPENDIX 3

THE MULTI-LAYER TRANSPARENT THIN FILMS ON SEMICONDUCTOR

To show normalised reflectance calculation for multi-layer thin films and substrate assembly, an example of eight layer thin films and silicon assembly is calculated. Fomulars in Sec.3.2 are successively applied. The result of this calculation are shown at same time in Fig.5.3b and in this Appendix.

Fig.5-3: The normalised reflectance calculation for a linearly inhomogenious thin film of thickness of 360 nm on Si. An eight layer subdivition is used.

$i := 0 .. 40 \qquad \lambda(i) := 400 + i \cdot 10$

$n1 := 1.35 \qquad t := 45$

$n2 := 1.3643$

$n3 := 1.3786$

$n4 := 1.3929$

$n5 := 1.4072 \qquad n8 := 1.45$

$n6 := 1.4215$

$n7 := 1.4358$

$$KH(i) := 0.030 - 0.1327 \cdot \frac{\lambda(i) - 550}{1000} + \frac{17}{75} \cdot \left[\frac{\lambda(i) - 550}{1000}\right]^2$$

$$KL(i) := 0.180 - 1.33 \cdot \frac{\lambda(i) - 400}{1000} + 1.99 \cdot \left[\frac{\lambda(i) - 400}{1000}\right]^2$$

$ks(i) := if(\lambda(i) < 550, KL(i), KH(i))$ (Silicon)

$$nH(i) := 4.090 - 3.6 \cdot \frac{\lambda(i) - 550}{1000} + 7 \cdot \left[\frac{\lambda(i) - 550}{1000}\right]^2$$

$$nL(i) := 5.060 - 9.867 \cdot \frac{\lambda(i) - 400}{1000} + 22.67 \cdot \left[\frac{\lambda(i) - 400}{1000}\right]^2$$ (Silicon)

$ns(i) := if(\lambda(i) < 550, nL(i), nH(i))$

$$\delta1(i) := \left[2 \cdot \pi \cdot n1 \cdot \frac{t}{\lambda(i)}\right] \qquad \delta2(i) := \left[2 \cdot \pi \cdot n2 \cdot \frac{t}{\lambda(i)}\right] \qquad \delta3(i) := \left[2 \cdot \pi \cdot n3 \cdot \frac{t}{\lambda(i)}\right]$$

$$\delta4(i) := \left[2 \cdot \pi \cdot n4 \cdot \frac{t}{\lambda(i)}\right] \qquad \delta5(i) := \left[2 \cdot \pi \cdot n5 \cdot \frac{t}{\lambda(i)}\right] \qquad \delta6(i) := \left[2 \cdot \pi \cdot n6 \cdot \frac{t}{\lambda(i)}\right]$$

$$\delta7(i) := \left[2 \cdot \pi \cdot n7 \cdot \frac{t}{\lambda(i)}\right] \qquad \delta8(i) := \left[2 \cdot \pi \cdot n8 \cdot \frac{t}{\lambda(i)}\right]$$

$a1(i) := \cos(\delta1(i)) \qquad a2(i) := \cos(\delta2(i)) \qquad a3(i) := \cos(\delta3(i))$

$a4(i) := \cos(\delta4(i)) \qquad a5(i) := \cos(\delta5(i)) \qquad a6(i) := \cos(\delta6(i))$

$a7(i) := \cos(\delta7(i)) \qquad a8(i) := \cos(\delta5(i))$

$$b1(i) := \frac{\sin(\delta1(i))}{n1} \qquad b2(i) := \frac{\sin(\delta2(i))}{n2} \qquad b3(i) := \frac{\sin(\delta3(i))}{n3}$$

$$b4(i) := \frac{\sin(\delta4(i))}{n4} \qquad b5(i) := \frac{\sin(\delta5(i))}{n5} \qquad b6(i) := \frac{\sin(\delta6(i))}{n6}$$

$$b7(i) := \frac{\sin(\delta7(i))}{n7} \qquad b8(i) := \frac{\sin(\delta8(i))}{n8}$$

```
c1(i) := n1·sin(δ1(i))        c2(i) := n2·sin(δ2(i))        c3(i) := n3·sin(δ3(i))
c4(i) := n4·sin(δ4(i))        c5(i) := n5·sin(δ5(i))        c6(i) := n6·sin(δ6(i))
c7(i) := n7·sin(δ7(i))        c8(i) := n8·sin(δ8(i))

d1(i) := a1(i)                d2(i) := a2(i)                d3(i) := a3(i)
d4(i) := a4(i)                d5(i) := a5(i)                d6(i) := a6(i)
d7(i) := a7(i)                d8(i) := a8(i)
a12(i) := a1(i)·a2(i) - b1(i)·c2(i)
b12(i) := a1(i)·b2(i) + b1(i)·d2(i)
c12(i) := c1(i)·a2(i) + d1(i)·c2(i)
d12(i) := d1(i)·d2(i) - c1(i)·b2(i)

a1_3(i) := a12(i)·a3(i) - b12(i)·c3(i)
b1_3(i) := a12(i)·b3(i) + b12(i)·d3(i)
c1_3(i) := c12(i)·a3(i) + d12(i)·c3(i)
d1_3(i) := d12(i)·d3(i) - c12(i)·b3(i)

a1_4(i) := a1_3(i)·a4(i) - b1_3(i)·c4(i)
b1_4(i) := a1_3(i)·b4(i) + b1_3(i)·d4(i)
c1_4(i) := c1_3(i)·a4(i) + d1_3(i)·c4(i)
d1_4(i) := d1_3(i)·d4(i) - c1_3(i)·b4(i)

a1_5(i) := a1_4(i)·a5(i) - b1_4(i)·c5(i)
b1_5(i) := a1_4(i)·b5(i) + b1_4(i)·d5(i)
c1_5(i) := c1_4(i)·a5(i) + d1_4(i)·c5(i)
d1_5(i) := d1_4(i)·d5(i) - c1_4(i)·b5(i)

a1_6(i) := a1_5(i)·a6(i) - b1_5(i)·c6(i)
b1_6(i) := a1_5(i)·b6(i) + b1_5(i)·d6(i)
c1_6(i) := c1_5(i)·a6(i) + d1_5(i)·c6(i)
d1_6(i) := d1_5(i)·d6(i) - c1_5(i)·b6(i)

a1_7(i) := a1_6(i)·a7(i) - b1_6(i)·c7(i)
b1_7(i) := a1_6(i)·b7(i) + b1_6(i)·d7(i)
c1_7(i) := c1_6(i)·a7(i) + d1_6(i)·c7(i)
d1_7(i) := d1_6(i)·d7(i) - c1_6(i)·b7(i)

a(i) := a1_7(i)·a8(i) - b1_7(i)·c8(i)
b(i) := a1_7(i)·b8(i) + b1_7(i)·d8(i)
c(i) := c1_7(i)·a8(i) + d1_7(i)·c8(i)
d(i) := d1_7(i)·d8(i) - c1_7(i)·b8(i)
```

$$r0(i) := \frac{(ns(i) - 1)^2 + ks(i)^2}{(ns(i) + 1)^2 + ks(i)^2}$$

$$y1(i) := \frac{ns(i) \cdot d(i) \cdot (a(i) + ks(i) \cdot b(i)) + (c(i) - ks(i) \cdot d(i)) \cdot (ns(i) \cdot b(i))}{(a(i) + ks(i) \cdot b(i))^2 + ns(i)^2 \cdot b(i)^2}$$

$$y2(i) := \frac{ns(i)^2 \cdot d(i) \cdot b(i) - (c(i) - ks(i) \cdot d(i)) \cdot (a(i) + ks(i) \cdot b(i))}{(a(i) + ks(i) \cdot b(i))^2 + ns(i)^2 \cdot b(i)^2}$$

$$r(i) := \frac{(1 - y1(i))^2 + y2(i)^2}{(1 + y1(i))^2 + y2(i)^2}$$

$$Rnom(i) := \frac{r(i)}{r0(i)}$$

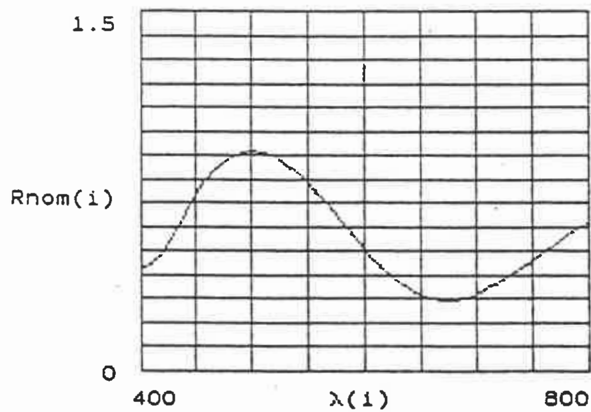

APPENDIX 4

THE SINGLE TRANSPARENT THIN FILMS ON TRANSPARENT SUBSTRATE

This appendix is a software for the normalised reflectance calculation of thin transparent films on transparent substrate. The R_{norm} is calculated using eguation (3.5)-(3.27) and assuming an semi-infinitive thick substrate. The R'_{norm} is calculated according to (3.27) and taking the back surface of the substrate into account.

Appendix.4-Fig.3.10

$i := 0 \,..40 \qquad d := 300 \quad \text{nm}$

$na := 1 \qquad nf(i) := 1.7$

$\lambda(i) := 400 + i \cdot 10 \qquad \text{nm}$

$$c := \begin{bmatrix} 0.6961663 \\ 0.0684043 \\ 0.4079426 \\ 0.1162414 \\ 0.8974794 \\ 9.8961610 \end{bmatrix} \qquad L(i) := \frac{\lambda(i)}{1000}$$

$$L1(i) := c_0 \cdot \frac{L(i)^2}{\left[L(i)^2 - \left(c_1\right)^2\right]}$$

$$L2(i) := c_2 \cdot \frac{L(i)^2}{\left[L(i)^2 - \left(c_3\right)^2\right]}$$

$$L3(i) := c_4 \cdot \frac{L(i)^2}{\left[L(i)^2 - \left(c_5\right)^2\right]}$$

$$ns(i) := (L1(i) + L2(i) + L3(i) + 1)^{\left[\frac{1}{2}\right]} \qquad (4.3)$$

$$\beta(i) := 2\cdot\pi\cdot nf(i)\cdot\frac{d}{\lambda(i)} \tag{3.5}$$

$$ks(i) := 0$$

$$r0(i) := \frac{\left[(ns(i) - na)^{2} + ks(i)^{2}\right]}{\left[(ns(i) + na)^{2} + ks(i)^{2}\right]} \tag{3.6}$$

$$m(i) := na\cdot\frac{ns(i)}{nf(i)}$$

$$m1(i) := \left[(m(i) - nf(i))^{2}\right]\cdot(\sin(\beta(i)))^{2}$$

$$m2(i) := \left[(m(i) + nf(i))^{2}\right]\cdot(\sin(\beta(i)))^{2}$$

$$r(i) := \left[\frac{\left[(na - ns(i))^{2}\cdot(\cos(\beta(i)))^{2} + m1(i)\right]}{\left[(na + ns(i))^{2}\cdot(\cos(\beta(i)))^{2} + m2(i)\right]}\right] \tag{3-16}$$

$$R0(i) := r0(i) + \left[\frac{r0(i)}{\left[1 - r0(i)^{2}\right]}\right]\cdot(1 - r0(i))^{2} \tag{3.24}$$

$$R(i) := r(i) + \left[\frac{r0(i)}{(1 - (r0(i) \cdot r(i)))}\right] \cdot (1 - r(i))^2$$

(3.21)

$$rnorm(i) := \frac{r(i)}{r0(i)}$$

(3.18)

$$Rnorm(i) := \frac{R(i)}{R0(i)}$$

(3.27)

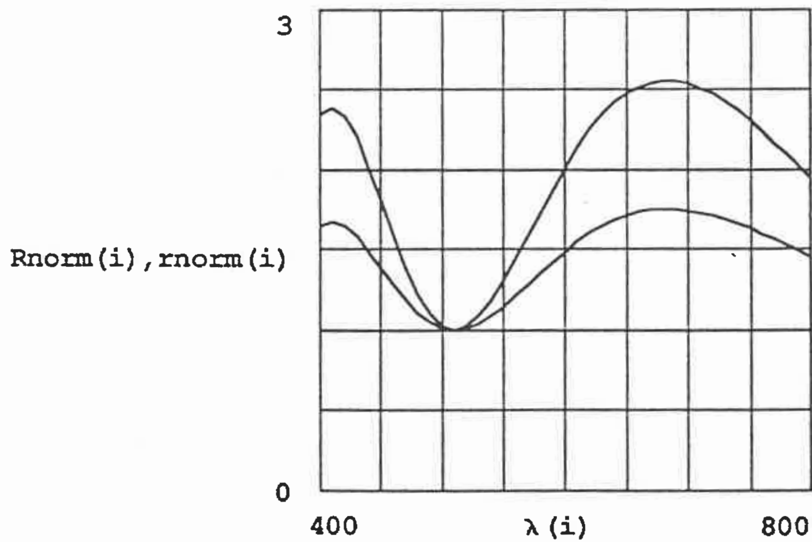

APPENDIX 5

THE SINGLE TRANSPARENT THIN FILMS ON AN ABSORBING SUBSTRATE

This is a software to simulate the normalised reflectance of a transparent thin film on an absorbing substrate. The substrate is thick enough that the rear surface do not contribute to the surface reflectance. The example of Fig. 12 is considered and equation (3.1) to (3.7) is used.

Appendix.5-Fig.3.12

i := 0 ..37   d := 857.5 nm

λ :=	ns :=	ks :=
400	5.570	0.387
403	5.493	0.355
407	5.349	0.313
416	5.164	0.255
425	5.009	0.211
431	4.916	0.194
439	4.791	0.170
449	4.682	0.149
456	4.615	0.131
462	4.553	0.131
473	4.466	0.120
480	4.416	0.094
488	4.367	0.079
496	4.320	0.073
504	4.277	0.066
512	4.235	0.060
521	4.196	0.056
530	4.159	0.043
539	4.123	0.048
544	4.106	0.044
554	4.073	0.032
559	4.042	0.032
569	3.997	0.027
579	3.969	0.030
596	3.943	0.025
608	3.918	0.024
626	3.893	0.022
639	3.870	0.018
660	3.847	0.016
674	3.815	0.014
689	3.796	0.013
697	3.778	0.012
721	3.761	0.011
738	3.745	0.010
756	3.728	0.009
775	3.721	0.008
795	3.705	0.007
800	3.688	0.006

$\lambda(i) := \lambda_i \qquad ns(i) := ns_i \qquad ks(i) := ks_i$

$na := 1$

$$c := \begin{bmatrix} 0.6961663 \\ 0.0684043 \\ 0.4079426 \\ 0.1162414 \\ 0.8974794 \\ 9.8961610 \end{bmatrix} \qquad L(i) := \frac{\lambda(i)}{1000}$$

$$L1(i) := c_0 \cdot \frac{L(i)^2}{L(i)^2 - {c_1}^2}$$

$$L2(i) := c_2 \cdot \frac{L(i)^2}{L(i)^2 - {c_3}^2}$$

$$L3(i) := c_4 \cdot \frac{L(i)^2}{\left[L(i)^2 - {c_5}^2\right]}$$

$$nf(i) := (L1(i) + L2(i) - L3(i))^{\left[\frac{1}{2}\right]} \qquad (4.3)$$

$$\beta(i) := 2 \cdot \pi \cdot nf(i) \cdot \frac{d}{\lambda(i)} \tag{3.5}$$

$$r12(i) := \frac{(nf(i) - na)}{(na + nf(i))} \tag{3.2}$$

$$p23(i) := \frac{\left[(ns(i) - nf(i))^{2} + ks(i)^{2}\right]^{0.5}}{\left[(nf(i) + ns(i))^{2} + ks(i)^{2}\right]^{0.5}} \tag{3.3}$$

$$R0(i) := \frac{\left[(ns(i) - na)^{2} + ks(i)^{2}\right]}{\left[(ns(i) + na)^{2} + ks(i)^{2}\right]} \tag{3.6}$$

$$\Phi23(i) := \operatorname{atan}\left[2 \cdot ks(i) \cdot \frac{nf(i)}{\left[ns(i)^{2} + ks(i)^{2} - nf(i)^{2}\right]}\right] \tag{3.4}$$

$$rp(i) := 2 \cdot r12(i) \cdot p23(i) \cdot \cos(\Phi23(i) + 2 \cdot \beta(i))$$

$$R(i) := \frac{\left[r12(i)^{2} + p23(i)^{2} + rp(i)\right]}{\left[1 + r12(i)^{2} \cdot p23(i)^{2} + rp(i)\right]} \tag{3.1}$$

$$\mathrm{Rnorm}(i) := \frac{R(i)}{R0(i)} \tag{3.7}$$

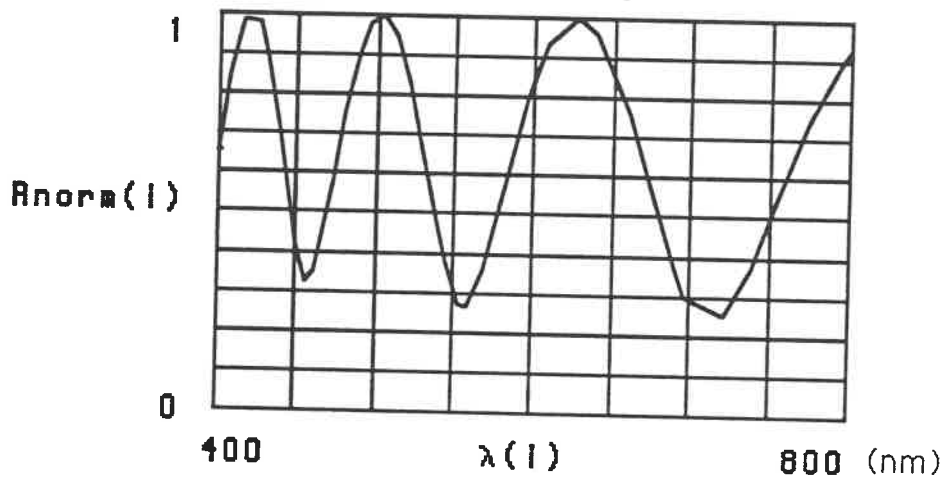

ÉCOLE POLYTECHNIQUE DE MONTRÉAL
3 9334 00210785 0